

Double-bracket quantum algorithms for quantum imaginary-time evolution

Marek Gluza,^{1,*} Jeongrak Son,¹ Bi Hong Tiang,¹ René Zander,²
Raphael Seidel,² Yudai Suzuki,^{3,4} Zoë Holmes,³ and Nelly H. Y. Ng^{1,5,†}

¹*School of Physical and Mathematical Sciences, Nanyang Technological University, 637371, Singapore*

²*Fraunhofer Institute FOKUS, Berlin, Germany*

³*Institute of Physics, Ecole Polytechnique Fédérale de Lausanne (EPFL), Lausanne, Switzerland*

⁴*Quantum Computing Center, Keio University, Hiyoshi 3-14-1, Kohoku-ku, Yokohama 223-8522, Japan*

⁵*Centre for Quantum Technologies, National University of Singapore, 3 Science Drive 2, 117543, Singapore*
(Dated: July 3, 2025)

Efficiently preparing approximate ground-states of large, strongly correlated systems on quantum hardware is challenging and yet nature is innately adept at this. This has motivated the study of thermodynamically inspired approaches to ground-state preparation that aim to replicate cooling processes via imaginary-time evolution. However, synthesizing quantum circuits that efficiently implement imaginary-time evolution is itself difficult, with prior proposals generally adopting heuristic variational approaches or using deep block encodings. Here, we use the insight that quantum imaginary-time evolution is a solution of Brockett's double-bracket flow and synthesize circuits that implement double-bracket flows coherently on the quantum computer. We prove that our Double-Bracket Quantum Imaginary-Time Evolution (DB-QITE) algorithm inherits the cooling guarantees of imaginary-time evolution. Concretely, each step is guaranteed to i) decrease the energy of an initial approximate ground-state by an amount proportion to the energy fluctuations of the initial state and ii) increase the fidelity with the ground-state. We provide gate counts for DB-QITE through numerical simulations in Qrisp which demonstrate scenarios where DB-QITE outperforms quantum phase estimation. Thus DB-QITE provides a means to systematically improve the approximation of a ground-state using shallow circuits.

Introduction.—Preparing ground-states of Hamiltonians is a fundamental task in quantum computation with wide-ranging applications from studying properties of materials [1] and chemicals [2] to solving optimization problems [3]. However, ground-state preparation is not only NP-hard [4] but also QMA-complete [5–8], and thus is a challenging problem even for quantum computers [9–12], let alone classical ones. Nevertheless, improvements on the computational efficiency over classical simulation is anticipated to be feasible with quantum processors [13–15]. In other words, the shift to quantum computing could offer a pathway to overcoming practical [16], conceptual [17] and fundamental [18, 19] challenges to the classical simulation of ground-states.

To date, various ground-state preparation algorithms have been proposed for both fault-tolerant [20–35] and near-term quantum computers [36–58]. Among these, a promising thermodynamic-inspired approach to cool an initial state $|\Psi_0\rangle$ with respect to a Hamiltonian \hat{H} is the *imaginary-time evolution* (ITE) defined by

$$|\Psi(\tau)\rangle = \frac{e^{-\tau\hat{H}}|\Psi_0\rangle}{\|e^{-\tau\hat{H}}|\Psi_0\rangle\|}. \quad (1)$$

Here τ is the ITE duration and the normalization involves the norm defined for any vector $|\Omega\rangle$ by $\| |\Omega\rangle \| = \sqrt{\langle\Omega|\Omega\rangle}$. ITE is guaranteed to converge to the ground-state $|\lambda_0\rangle$ of \hat{H} in case the initial overlap with the ground-state is non-zero [59].

We distinguish ITE from *quantum imaginary-time evolution* (QITE) [23, 36–43] in that ITE is defined by the normalized action of a non-unitary propagator and QITE is the

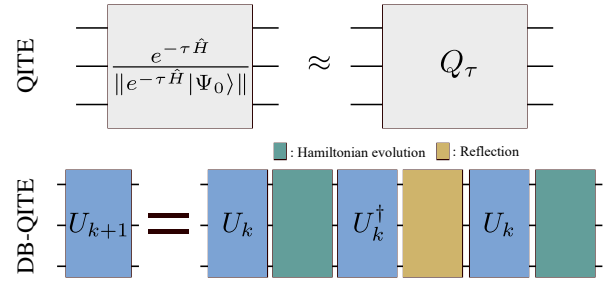


FIG. 1. Double-bracket Quantum Imaginary-Time Evolution (DB-QITE). We propose a new quantum algorithm to implement imaginary-time evolution (ITE). To implement the Quantum Imaginary-Time Evolution (QITE) unitary Q_τ , we utilize a Double-Bracket Quantum Algorithm (DBQA) and show that QITE can be recursively compiled using Hamiltonian evolution and reflection gates.

implementation of ITE by explicitly using a unitary Q_τ such that $|\Psi(\tau)\rangle = Q_\tau|\Psi_0\rangle$. Finding the unitaries that implement the ITE states $|\Psi(\tau)\rangle$ is not straightforward. One family of approaches use a hybrid quantum-classical optimization loop to learn Q_τ [36–42]. This can yield compressed circuits by fine-tuning to individual input instances, but scaling to large problem sizes is generally inhibited by growing requirements on measurement precision [60, 61]. Another approach is to extend the system size and approximate the non-unitary propagator with qubitization [23]. However, the overheads of implementing so-called block-encodings preclude flexible near-term experiments. In other words, constructing efficient circuits for QITE remains an open problem.

In this work, we offer a resolution to this problem by drawing on the observation that ITE is a solution to well-studied differential equations known as *double-bracket flows*

* marekludwik.gluza@ntu.edu.sg

† nelly.ng@ntu.edu.sg

(DBF) [62–79]. DBFs are appealing for quantum computation because their solutions arise from unitaries, a feature recently exploited for quantum circuit synthesis by means of double-bracket quantum algorithms (DBQA) [32, 53, 54]. DBFs come with local optimality proofs in that they implement gradient flows [62–66, 80] and these are known to converge exponentially fast to their fixed points [81]. Accordingly, DBQAs have recently been shown to provide a compilation procedure which is able to significantly improve on circuits optimized by brute-force [53]. Here we introduce an algorithm, termed *double-bracket QITE* (DB-QITE), that implements steps of gradient flows *coherently* on a quantum computer [32], without resorting to classical computations, heuristic hybrid quantum-classical variational methods, or block encodings. Instead, the DBQA approach produces recursive quantum circuits which at every step approximates the DBF of ITE, as sketched in Fig. 1.

Crucially, DB-QITE inherits the cooling properties of ITE, as summarized in Table I. Namely, we provide rigorous guarantees that DB-QITE systematically lowers the energy of a state and increases its fidelity with the ground-state. As we will see, DB-QITE has a similar cooling rate as ITE, with the rate larger for quantum states with high energy fluctuations. Moreover, a single step of DB-QITE is guaranteed to increase the fidelity with the ground-state by an amount proportional to the initial fidelity with the ground-state and the spectral gap of the target Hamiltonian. Furthermore, as our bounds hold for any input state (in contrast to Ref. [82]) this argument can be applied iteratively to show that the DB-QITE unitaries yield states which converge exponentially fast in the number of iterations to the ground-state. Given this recursive structure, the circuit depths required to implement DB-QITE grow exponentially with the number of steps. As we show numerically, optimizing the free parameter of step durations reduces the number of iterations to a level competitive with state-of-the-art methods.

Thus DB-QITE provides a means to systematically reduce the energy of an approximate ground-state. We expect our algorithm to be used both as a standalone ground-state preparation method in the early fault-tolerant era, as well as in conjunction with more established [20–24] and heuristic approaches [36–40, 55, 56, 83] to ground-state preparation.

Fluctuation-refrigeration relation of ITE.—ITE defined in Eq. (1) satisfies [59]

$$\partial_\tau |\Psi(\tau)\rangle = -(\hat{H} - E(\tau))|\Psi(\tau)\rangle \quad (2)$$

with the energy $E(\tau) = \langle \Psi(\tau) | \hat{H} | \Psi(\tau) \rangle$. Under such evolutions, the state is guaranteed to converge to the ground-state of the Hamiltonian in the limit of $\tau \rightarrow \infty$ as long as the initial state $|\Psi_0\rangle$ has some non-zero overlap to the ground-state [59]. This fact has driven the exploration of how to implement ITE on classical [84] and quantum computers [36–42]. From Eq. (2), a direct computation (see Supplemental Materials II B) gives

$$\partial_\tau E(\tau) = -2V(\tau), \quad (3)$$

where $V(\tau) = \langle \Psi(\tau) | (\hat{H} - E(\tau))^2 | \Psi(\tau) \rangle$ is the energy fluctuation (the operator variance of the Hamiltonian). It follows

	Fluctuation-Refrigeration Relation	Fidelity
ITE	$\partial_\tau E(\tau) = -2V(\tau)$ [Eq. (3)]	$1 - \mathcal{O}(e^{-2\tau\Delta})$ [Eq. (56)]
DB-QITE	$E_{k+1} \leq E_k - 2s_k V_k + \mathcal{O}(s_k^2)$ [Theorem 1]	$1 - \mathcal{O}(q^k)$ [Theorem 2]

TABLE I. **Energy reduction guarantees for DB-QITE.** It is known that the ITE can lower the energy $E(\tau)$ by an amount proportional to the energy fluctuation $V(\tau)$. We call this a fluctuation-refrigeration relation. ITE is also guaranteed to improve the fidelity to the ground-state exponentially in the imaginary-time τ . Similarly to ITE, DB-QITE agrees with the amount of energy reduction $E_{k+1} - E_k$ up to corrections of order $\mathcal{O}(s_k^2)$, and improves the fidelity exponentially fast in the time of algorithm iterations k .

that higher energy fluctuations in the state lead to a faster energy decrease. We call this a *fluctuation-refrigeration relation*, and will show that an analogous relation holds for the quantum circuits that we will propose to approximate ITE.

ITE is a solution of DBF.—We next observe that ITE Eq. (2) can be rewritten as

$$\partial_\tau |\Psi(\tau)\rangle = [\Psi(\tau), \hat{H}] |\Psi(\tau)\rangle, \quad (4)$$

where $\Psi(\tau) = |\Psi(\tau)\rangle\langle\Psi(\tau)|$ is the density matrix of the ITE state and $[A, B] = AB - BA$ is the commutator [85]. In terms of the density matrix $\Psi(\tau)$, we get

$$\frac{\partial \Psi(\tau)}{\partial \tau} = [[\Psi(\tau), \hat{H}], \Psi(\tau)]. \quad (5)$$

This is exactly the form of the well-studied Brockett’s DBF [66]. In End Matter, we review its relation to Riemannian gradient descent on unitary manifolds and state the relevant cost functions. Given Eq. (5), these results from DBF theory now apply to QITE and in essence signify its local optimality.

QITE from ITE DBF.—The difficulty of implementing ITE on quantum computers lies in the non-unitarity of the propagator in Eq. (1) and its state-dependence in Eq. (2). The challenge thus lies in circuit synthesis of unitaries Q_τ satisfying

$$|\Psi(\tau)\rangle \approx Q_\tau |\Psi_0\rangle. \quad (6)$$

This transition from non-unitary ITE propagation in Eq. (1) to unitary implementation in Eq. (6) is termed QITE. Intuitively, we have from Eq. (4) that for short durations $\Delta\tau$,

$$|\Psi(\Delta\tau)\rangle \approx e^{\Delta\tau[\Psi(0), \hat{H}]} |\Psi_0\rangle. \quad (7)$$

Thus, writing ITE as a DBF directly results in a proposal for QITE, at least for short durations. It is not straightforward to rigorously quantify the approximation in Eq. (7), see Refs. [32, 86]. Nevertheless, we show in Prop. 11 of App. III B that the energy decrease of this dynamics agrees with Eq. (3) up to

corrections of order $\mathcal{O}(\Delta\tau^2)$. Motivated by this, we initialize a recursion by the initial state $|\sigma_0\rangle = |\Psi_0\rangle$ and define

$$|\sigma_{k+1}\rangle = e^{s_k[\langle\sigma_k|\hat{H}|\sigma_k\rangle]}|\sigma_k\rangle. \quad (8)$$

Here, we denote the time step size in the $(k+1)$ -th step as s_k . Rigorous results from Refs. [62, 63, 65, 66] apply to Eq. (8) and prove convergence to the ground-state as $k \rightarrow \infty$. The recursion in Eq. (8) provides an explicit recipe for QITE unitaries in Eq. (6). However, further circuit synthesis is needed as $e^{s_k[\langle\sigma_k|\hat{H}|\sigma_k\rangle]}$ is challenging to execute directly on a quantum computer.

DB-QITE circuit synthesis.—Next, we compile QITE unitaries as quantum circuit using the group commutator iterations first introduced in Ref. [32]. In the context of QITE we define the group commutator of any density matrix Ω by

$$G_s(\Omega) = e^{i\sqrt{s}\hat{H}} e^{i\sqrt{s}\Omega} e^{-i\sqrt{s}\hat{H}} e^{-i\sqrt{s}\Omega}. \quad (9)$$

The Supplemental Materials of Ref. [32] show that

$$G_s(\Omega) = e^{s[\Omega, \hat{H}]} + \mathcal{O}(s^{3/2}), \quad (10)$$

see Refs. [87–89] for further context. In order to formulate the circuit synthesis for DB-QITE we first notice that when applying $G_s(|\Omega\rangle\langle\Omega|)$ to $|\Omega\rangle$ there is a cancellation and find

$$e^{i\sqrt{s}}G_s(|\Omega\rangle\langle\Omega|)|\Omega\rangle = e^{i\sqrt{s}\hat{H}} e^{i\sqrt{s}|\Omega\rangle\langle\Omega|} e^{-i\sqrt{s}\hat{H}} |\Omega\rangle. \quad (11)$$

This allows us to arrive at the following DB-QITE states

$$|\omega_{k+1}\rangle = e^{i\sqrt{s_k}\hat{H}} e^{i\sqrt{s_k}|\omega_k\rangle\langle\omega_k|} e^{-i\sqrt{s_k}\hat{H}} |\omega_k\rangle. \quad (12)$$

Finally, let U_k denote the circuit to prepare $|\omega_k\rangle$ from a trivial reference state $|0\rangle$, i.e., $|\omega_k\rangle = U_k|0\rangle$. We can now use unitarity to simplify $e^{i\sqrt{s_k}|\omega_k\rangle\langle\omega_k|} = U_k e^{i\sqrt{s_k}|0\rangle\langle 0|} U_k^\dagger$ and arrive at a recursive formula for DB-QITE circuit synthesis

$$U_{k+1} = e^{i\sqrt{s_k}\hat{H}} U_k e^{i\sqrt{s_k}|0\rangle\langle 0|} U_k^\dagger e^{-i\sqrt{s_k}\hat{H}} U_k. \quad (13)$$

Step $k=0$ involves U_0 which is used to define $|\omega_0\rangle := U_0|0\rangle$. When $U_0 = I$ then DB-QITE operates as standalone and when $|\omega_0\rangle$ approximates the ground-state $|\lambda_0\rangle$ of the input Hamiltonian \hat{H} then U_0 is a warm-start with subsequent steps of DB-QITE continuing to leverage on U_0 implicitly. Fig. 1 summarizes this recursive circuit synthesis and the compilation of DB-QITE is completed by invoking known efficient schemes for Hamiltonian simulation [90–94] and reflections [95–97].

Analysis of DB-QITE.—Similarly to ITE, DB-QITE obeys a fluctuation-refrigeration relation where the energy reduction in every step is bounded by the energy fluctuations as in Eq. (3).

Theorem 1. Fluctuation-refrigeration relation. *The average energy $E_k := \langle\omega_k|\hat{H}|\omega_k\rangle$ of the states $|\omega_k\rangle := U_k|0\rangle$, where U_k is defined recursively in Eq. (13), obeys*

$$\frac{E_{k+1} - E_k}{s_k} \leq -2V_k + \mathcal{O}(s_k) \quad (14)$$

where $V_k := \langle\omega_k|\hat{H}^2|\omega_k\rangle - E_k^2$ is the variance of the energy in state $|\omega_k\rangle$.

We prove this statement in Theorem 16 in App. IV. This shows that in every step of DB-QITE cooling rate matches the cooling rate of continuous ITE up to $\mathcal{O}(s_k^2)$. Moreover, we give sufficient conditions on s_k such that the higher order terms $\mathcal{O}(s_k^2)$ do not overhaul the first order cooling.

The energy reduction of DB-QITE quantified in Eq. (14) is warranted by non-negativity of the energy variances $V_k > 0$. However, Eq. (14) does not yet exclude the possibility of converging to an excited energy eigenstate. Next, we will show that such scenarios do not occur. Concretely, as proven in App. IV, the following theorem holds.

Theorem 2. Ground-state fidelity increase guarantee. *Suppose DB-QITE is initialized with a non-zero initial ground-state overlap F_0 . Let \hat{H} be a Hamiltonian with a unique ground-state $|\lambda_0\rangle$ and $\lambda_0 = 0$, spectral gap Δ and spectral radius $\|\hat{H}\| \geq 1$. Let U_0 be an arbitrary unitary and set*

$$s = \frac{\Delta}{12\|\hat{H}\|^3}. \quad (15)$$

The states $|\omega_k\rangle := U_k|0\rangle$, where U_k is defined recursively in Eq. (13), satisfy

$$F_{k+1} := |\langle\lambda_0|\omega_{k+1}\rangle|^2 \geq F_k \left(1 + \frac{(1 - F_k)\Delta^2}{12\|\hat{H}\|^3} \right) \geq 1 - q^k \quad (16)$$

where $q = 1 - sF_0\Delta$.

This result shows that DB-QITE systematically synthesizes circuits that improve on previous circuits to prepare a better approximation to the ground-state. In particular, the first step is guaranteed to increase the fidelity with the ground-state by $F_0(1 - F_0)\Delta^2/12\|\hat{H}\|^3$ where F_0 is the fidelity of the initial guess state $U_0|0\rangle$ and Δ is the spectral gap. Moreover, subsequent iterations are guaranteed to further increase the fidelity to the ground-state and avoid converging to excited states (as could be consistent with Theorem 1). Hence DB-QITE provides a means of systematically preparing states with increased fidelity with the ground-state.

System-size scaling of DB-QITE.—Resources required to run DB-QITE grow with system size but for a gapped local Hamiltonian the improvement from a single step of DB-QITE only degrades polynomially with system size L . Namely, it is clear from the formal statement of Theorem 1 (i.e., Theorem 16 in App. IV) that a polynomially decreasing s suffices to ensure the inequality in Eq. (14) holds strictly and so for constant fluctuations V_k the energy gain reduces only polynomially. Similarly, if $\Delta \in \Theta(1)$ and $\|\hat{H}\| \in \Theta(L)$ then the fidelity gain for a constant initial fidelity is only reduced by a polynomial factor. Moreover, the circuit depth required to implement a single iteration of DB-QITE only increases polynomially with system size (inline with the standard scaling of reflections and Hamiltonian simulation) and thus our circuit scalings for a single iteration of DB-QITE are favorable. In the End Matter we further discuss the scaling for consecutive

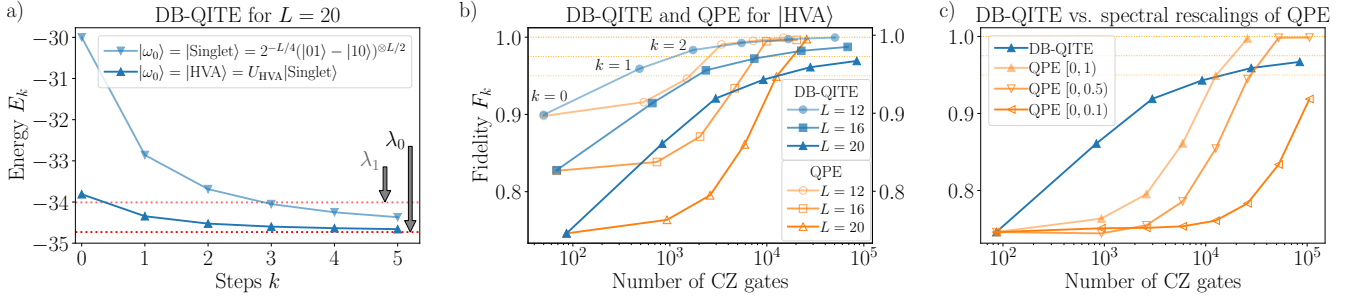


FIG. 2. Numerical benchmarks for the 1d Heisenberg model. (a) DB-QITE for $L = 20$ qubits starting with either a product of singlets $|\text{Singlet}\rangle$ or a low-depth variationally learnt ‘warm-start’ state $|\text{HVA}\rangle$ based on Refs. [98–100]. When extending s_k , just a handful of steps allows to reach $E_k \ll \lambda_1$. (b) Two DB-QITE steps yield fidelities $F_2 \geq 95\%$ for $L = 12$ and $F_2 \geq 90\%$ for $L = 20$ by using approximately 2×10^3 CZ gates. QPE (orange) outperforms DB-QITE (blue) only when fault-tolerant execution allows for circuits with more than 10^4 CZ gates. In contrast, DB-QITE achieves high fidelity using fewer gates and more homogeneous circuits (See App. V for details). (c) QPE ideally uses a rescaled Hamiltonian $\hat{H}' = (\hat{H} - \lambda_0 \mathbb{1})/(\|\hat{H}\| - \lambda_0)$, but overestimating $\|\hat{H}\|$ (e.g., by a factor of 2) significantly increases QPE runtime. In such cases, DB-QITE can attain fidelity $F_4 \approx 95\%$ more efficiently.

iterations of DB-QITE which are less favorable due to DB-QITE’s recursive structure but next we provide numerical evidence that these scalings carry less weight when using larger step sizes s_k than prescribed by worst-case bounds in Eq. (15).

Numerical simulations of DB-QITE.—We performed numerical simulations for the Heisenberg model with up to $L = 20$ qubits and optimized s_k by choosing the value giving the largest energy gain among 20 evaluations of E_k obtained with trial values for s_k . Fig. 2a) shows that this increases energy gain beyond Eq. (15) and the linearization in Eq. (14); each DB-QITE step removes about half of the excess energy. Quantitatively, DB-QITE reaches fidelity $F_2 \geq 90\%$ for $k = 2$ steps using less than $N_{\text{CZ}} \leq 3 \times 10^3$ CZ gates and $N_{\text{U3}} \leq 4.8 \times 10^3$ single-qubit gates. Roughly half of this runtime suffices to achieve $F_2 \geq 95\%$ for $L = 12$ qubits. These gate-counts are within reach of existing hardware [101–103]. The circuit compilation is automated in the Qrisp programming language [104] and the cost of implementing reflections is reduced by involving auxiliary qubits, see App. V for details. Qrisp allows us to compile circuits for $L \gg 20$ albeit without computing energy and fidelity gains. If the same amount of Trotter-Suzuki steps in Hamiltonian simulation remains appropriate for $L = 50$ then $k = 1$ step of DB-QITE will require $N_{\text{U3}} \approx 3.4 \times 10^3$ single-qubit gates and $N_{\text{CZ}} \approx 2 \times 10^3$ CZ gates while $k = 2$ requires $N_{\text{U3}} \approx 1.2 \times 10^4$ and $N_{\text{CZ}} \approx 7 \times 10^3$.

The main limitation of current large scale quantum devices is the fidelity of two-qubit gates, limiting the maximum realistically implementable CZ gates to $N_{\text{CZ}} \lesssim 10^3$ [101]. Fig. 2b) shows that if executed experimentally now, DB-QITE outperforms the canonical quantum phase estimation (QPE) variant reviewed in Ref. [21], a paradigmatic example of ground-state preparation algorithms geared towards fault-tolerant hardware [20–33]. Specifically, when $N_{\text{CZ}} \lesssim 10^3$, DB-QITE yields $F_1 \geq 95\%$ for $L = 12$ and $F_2 \geq 85\%$ for $L = 20$ while QPE is limited to only 1 digit of precision and offers almost no improvement over initialization with $F_0 \approx 75\%$.

DB-QITE continues to outperform QPE when more CZ

gates are available up until requiring fault-tolerance at around $N_{\text{CZ}} \gtrsim 10^4$. This facilitates about 5 digits of precision in QPE and better fidelities than DB-QITE. However, it is likely a substantial resource underestimate that QPE would in practice reach such fidelities for $N_{\text{CZ}} \gtrsim 10^4$ because we had to make strong assumptions to achieve that: *i)* knowing the energy of the ground-state and highest-excited state, *ii)* all-to-all interactions and *iii)* perfect measurement calibration. In Fig. 2b), we computed λ_0 and $\|\hat{H}\|$ by exact diagonalization for $L \leq 20$ but in general these tasks are computationally intractable. Fig. 2c) highlights that even for $N_{\text{CZ}} \gtrsim 10^4$, DB-QITE will continue to compete with QPE’s performance: An overestimate of $\|\hat{H}\|$ by a factor 2 means that QPE needs 6 auxiliary qubits to reach precision outperforming DB-QITE. For a factor of 10, we found that 7 auxiliary qubits do not suffice. DB-QITE’s independence of rescalings is a general advantage as methods involving block-encodings rely on such rescalings too [20, 105, 106].

Discussion.—The fact that imaginary-time evolution (ITE) is a solution to double-bracket flows (DBFs) implies that ITE is an optimal gradient descent method in the sense of being a steepest-descent flow [62, 63, 65, 66, 80]. The local optimality of DBFs has previously been investigated in the context of circuit compilation [52] and has motivated tangent-space methods crucial for tensor network simulations [107–113]. However, these studies involved classical processing at its core. Here, rather than resorting to classical computations or heuristic hybrid quantum-classical variational methods [60, 61, 114–117], we took the radically different approach of implementing DBFs *coherently* on the quantum computer [32].

Concretely, we propose the double-bracket quantum imaginary-time evolution (DB-QITE) algorithm which exploits the connection of DBF and ITE to obtain unitaries in Eq. (13) guaranteed to reduce the energy. This is achieved through a recursive application of the group commutator. DB-QITE involves forward and backward evolutions under the target Hamiltonian, interspersed with reflection operations and the initial state preparation unitaries. These ingredients are similar to bang-bang protocols for quantum control [118–

[120]. However, while this quantum control paradigm is usually restricted to small systems, DB-QITE can be viewed as a quantum many-body echo protocol [121]. Our strategies can have implications for fields other than quantum computing which also employ ITE, e.g. path-integral optimization used to study holographic complexity in AdS/CFT correspondence [122, 123].

DB-QITE inherits characteristics of ITE for ground-state preparation. Specifically, Thm. 2 establishes that states prepared via DB-QITE are guaranteed to converge towards the ground-state exponentially in the number of steps and Eq. (14) shows that DB-QITE has, to first order, the same energy reduction rate as ITE. Both properties are ramifications of DB-QITE's rooting in gradient flow theory [62, 63, 65, 66, 81]. That the cooling rate of QITE is, similarly to ITE, determined by the energy fluctuations in the initial state is in line with the physical intuition that fast control of a system needs coherence in the energy basis [124, 125]. This suggests the possibility to derive quantum speed limits for cooling with a measurable metric that involves energy fluctuations.

While each step k of DB-QITE is guaranteed to increase the ground-state fidelity, the circuit depth grows as $\mathcal{O}(3^k)$. Nonetheless, we provided numerical evidence that optimization of step durations s_k leads to circuits within reach of existing quantum hardware and yielding high-fidelity approximations to ground-states of the Heisenberg models. We found that for QPE to outperform DB-QITE, it required unrealistic assumptions, such as perfect knowledge of the spectrum and all-to-all connectivity. We also found that when large circuit depths are available, then QPE's success probability is im-

proved by initializing from a DB-QITE warm-start. We expect DB-QITE warm-starts will be useful in conjunction with other methods too [20–33, 40]. Our numerical results suggest that performing even a handful more DB-QITE steps is useful and this could be achieved by quantum dynamic programming [126]. In general, to keep the runtime low, it is essential to optimize the step sizes s_k [32, 53, 54, 127] which can be done based on measurements of the energy mean. We conclude that DB-QITE, with its rigorous convergence guarantee and tractable gate counts, offers a refined pathway for ground-state preparation on large-scale quantum hardware.

Code availability. The source code to reproduce all numerical simulations in Qrisp and the figures is available openly at <https://github.com/renezander90/DB-QITE>.

Acknowledgments. We thank David Gosset for sharing his observation about QITE in Eq. (4) which he discovered while working on Ref. [82]. Insightful discussions with José Ignacio Latorre and Alexander Jahn are gratefully acknowledged.

MG, JS, BHT and NN are supported by the start-up grant of the Nanyang Assistant Professorship at the Nanyang Technological University in Singapore. MG has also been supported by the Presidential Postdoctoral Fellowship of the Nanyang Technological University in Singapore. ZH acknowledges support from the Sandoz Family Foundation-Monique de Meuron program for Academic Promotion. RS and RZ are supported by European Union's Horizon Europe research and innovation program under grant agreement no. 101119547.

-
- [1] Y. Alexeev, M. Amsler, M. A. Barroca, S. Bassini, T. Battelle, D. Camps, D. Casanova, Y. J. Choi, F. T. Chong, C. Chung, *et al.*, Quantum-centric supercomputing for materials science: A perspective on challenges and future directions, *Future Generation Computer Systems* **160**, 666 (2024).
 - [2] S. McArdle, S. Endo, A. Aspuru-Guzik, S. C. Benjamin, and X. Yuan, Quantum computational chemistry, *Rev. Mod. Phys.* **92**, 015003 (2020).
 - [3] K. Blekos, D. Brand, A. Ceschini, C.-H. Chou, R.-H. Li, K. Pandya, and A. Summer, A review on quantum approximate optimization algorithm and its variants, *Physics Reports* **1068**, 1 (2024).
 - [4] F. Barahona, On the computational complexity of Ising spin glass models, *J. Phys. A* **15**, 3241 (1982).
 - [5] D. Aharonov, D. Gottesman, S. Irani, and J. Kempe, The power of quantum systems on a line, *Commun. Math. Phys.* **287**, 41 (2009).
 - [6] J. Kempe, A. Kitaev, and O. Regev, The complexity of the local Hamiltonian problem, *SIAM J. of Comp.* **35**, 1070 (2006).
 - [7] J. Bausch, T. Cubitt, and M. Ozols, The complexity of translationally-invariant spin chains with low local dimension, arXiv preprint arXiv:1605.01718 (2016).
 - [8] J. Kempe and O. Regev, 3-local Hamiltonian is QMA-complete, *Quantum Inf. Comput.* **3**, 258 (2003).
 - [9] T. J. Osborne, Hamiltonian complexity, *Rep. Prof. Phys.* **75**, 022001 (2012).
 - [10] S. Gharibian, Y. Huang, Z. Landau, S. W. Shin, *et al.*, Quantum Hamiltonian complexity, *Found. Tr. Th. Comp. Sc.* **10**, 159 (2015).
 - [11] D. Aharonov, I. Arad, Z. Landau, and U. Vazirani, ArXiv:1011.3445.
 - [12] D. Aharonov and T. Naveh, Quantum NP – a survey, arXiv: quant-ph/0210077 (2002).
 - [13] C. Cade, L. Mineh, A. Montanaro, and S. Stanisic, Strategies for solving the Fermi-Hubbard model on near-term quantum computers, *Phys. Rev. B* **102**, 235122 (2020).
 - [14] D. Wu, R. Rossi, F. Vicentini, N. Astrakhantsev, F. Becca, X. Cao, J. Carrasquilla, F. Ferrari, A. Georges, M. Hibat-Allah, *et al.*, Variational benchmarks for quantum many-body problems, *Science* **386**, 296 (2024).
 - [15] A. Auffèves, Quantum technologies need a quantum energy initiative, *PRX Quantum* **3**, 020101 (2022).
 - [16] P. Nataf and F. Mila, Exact Diagonalization of Heisenberg $SU(N)$ Models, *Phys. Rev. Lett.* **113**, 127204 (2014).
 - [17] R. P. Feynman, Simulating physics with computers, *Int. J. Th. Phys.* **21**, 467 (1982).
 - [18] R. Impagliazzo and R. Paturi, Complexity of k-sat, in *Proceedings. Fourteenth Annual IEEE Conference on Computational Complexity (Formerly: Structure in Complexity Theory Conference) (Cat.No.99CB36317)* (1999) pp. 237–240.
 - [19] V. Strassen *et al.*, Gaussian elimination is not optimal, *Numerische mathematik* **13**, 354 (1969).
 - [20] L. Lin and Y. Tong, Near-optimal ground state preparation, *Quantum* **4**, 372 (2020).

- [21] Y. Ge, J. Tura, and J. I. Cirac, Faster ground state preparation and high-precision ground energy estimation with fewer qubits, *Journal of Mathematical Physics* **60**, 022202 (2019).
- [22] A. Gilyén, Y. Su, G. H. Low, and N. Wiebe, Quantum singular value transformation and beyond: exponential improvements for quantum matrix arithmetics, in *Proceedings of the 51st Annual ACM SIGACT Symposium on Theory of Computing* (2019) pp. 193–204.
- [23] T. de Lima Silva, M. M. Taddei, S. Carrazza, and L. Aolita, *Fragmented imaginary-time evolution for early-stage quantum signal processors* (2023), [arXiv:2110.13180 \[quant-ph\]](https://arxiv.org/abs/2110.13180).
- [24] Y. Dong, L. Lin, and Y. Tong, Ground-state preparation and energy estimation on early fault-tolerant quantum computers via quantum eigenvalue transformation of unitary matrices, *PRX Quantum* **3**, 10.1103/prxquantum.3.040305 (2022).
- [25] E. N. Epperly, L. Lin, and Y. Nakatsukasa, A theory of quantum subspace diagonalization, *SIAM Journal on Matrix Analysis and Applications* **43**, 1263–1290 (2022).
- [26] K. Temme, T. J. Osborne, K. G. Vollbrecht, D. Poulin, and F. Verstraete, Quantum metropolis sampling, *Nature* **471**, 87 (2011).
- [27] A. Y. Kitaev, *Quantum measurements and the abelian stabilizer problem* (1995), [arXiv:quant-ph/9511026 \[quant-ph\]](https://arxiv.org/abs/quant-ph/9511026).
- [28] G. Brassard, P. Hoyer, M. Mosca, and A. Tapp, Quantum amplitude amplification and estimation, *Contemporary Mathematics* **305**, 53 (2002).
- [29] K. C. Tan, D. Bowmick, and P. Sengupta, *Quantum stochastic series expansion methods* (2020), [arXiv:2010.00949](https://arxiv.org/abs/2010.00949).
- [30] G. H. Low and I. L. Chuang, Hamiltonian Simulation by Qubitization, *Quantum* **3**, 163 (2019).
- [31] D. Wecker, B. Bauer, B. K. Clark, M. B. Hastings, and M. Troyer, Gate-count estimates for performing quantum chemistry on small quantum computers, *Phys. Rev. A* **90**, 022305 (2014).
- [32] M. Gluza, Double-bracket quantum algorithms for diagonalization, *Quantum* **8**, 1316 (2024).
- [33] D. Poulin and P. Wocjan, Sampling from the thermal quantum gibbs state and evaluating partition functions with a quantum computer, *Phys. Rev. Lett.* **103**, 220502 (2009).
- [34] D. Motlagh, M. S. Zini, J. M. Arrazola, and N. Wiebe, Ground state preparation via dynamical cooling, *arXiv preprint arXiv:2404.05810* <https://doi.org/10.48550/arXiv.2404.05810> (2024).
- [35] W. Kirby, M. Motta, and A. Mezzacapo, Exact and efficient Lanczos method on a quantum computer, *Quantum* **7**, 1018 (2023).
- [36] N. Gomes *et al.*, Adaptive variational quantum imaginary time evolution approach for ground state preparation, *Advanced Quantum Technologies* **4**, 2100114 (2021).
- [37] S. McArdle *et al.*, Variational ansatz-based quantum simulation of imaginary time evolution, *npj Quantum Information* **5**, 75 (2019).
- [38] H. Nishi, T. Kosugi, and Y.-i. Matsushita, Implementation of quantum imaginary-time evolution method on NISQ devices by introducing nonlocal approximation, *npj Quantum Information* **7**, 85 (2021).
- [39] K. Yeter-Aydeniz, R. C. Pooser, and G. Siopsis, Practical quantum computation of chemical and nuclear energy levels using quantum imaginary time evolution and Lanczos algorithms, *npj Quantum Information* **6**, 63 (2020).
- [40] M. Motta, C. Sun, A. T. Tan, M. J. O’Rourke, E. Ye, A. J. Minnich, F. G. Brandao, and G. K. Chan, Determining eigenstates and thermal states on a quantum computer using quantum imaginary time evolution, *Nature Physics* **16**, 205 (2020).
- [41] K. Yeter-Aydeniz, B. T. Gard, J. Jakowski, S. Majumder, G. S. Barron, G. Siopsis, T. S. Humble, and R. C. Pooser, Benchmarking quantum chemistry computations with variational, imaginary time evolution, and Krylov space solver algorithms, *Advanced Quantum Technologies* **4**, 2100012 (2021).
- [42] N. Gomes, F. Zhang, N. F. Berthussen, C.-Z. Wang, K.-M. Ho, P. P. Orth, and Y. Yao, Efficient step-merged quantum imaginary time evolution algorithm for quantum chemistry, *Journal of Chemical Theory and Computation* **16**, 6256 (2020).
- [43] Y. Huang, Y. Shao, W. Ren, J. Sun, and D. Lv, Efficient quantum imaginary time evolution by drifting real-time evolution: An approach with low gate and measurement complexity, *Journal of Chemical Theory and Computation* **19**, 3868 (2023).
- [44] K. Hejazi, M. Motta, and G. K.-L. Chan, Adiabatic quantum imaginary time evolution, *Phys. Rev. Res.* **6**, 033084 (2024).
- [45] L. Lin and Y. Tong, Heisenberg-Limited Ground-State Energy Estimation for Early Fault-Tolerant Quantum Computers, *PRX Quantum* **3**, 010318 (2022).
- [46] R. LaRose, A. Tikku, É. O’Neel-Judy, L. Cincio, and P. J. Coles, Variational quantum state diagonalization, *npj Quantum Information* **5**, 1 (2019).
- [47] J. Zeng, C. Cao, C. Zhang, P. Xu, and B. Zeng, A variational quantum algorithm for hamiltonian diagonalization, *Quantum Science and Technology* **6**, 045009 (2021).
- [48] R. M. Parrish and P. L. McMahon, *Quantum filter diagonalization: Quantum eigendecomposition without full quantum phase estimation* (2019), [arXiv:1909.08925 \[quant-ph\]](https://arxiv.org/abs/1909.08925).
- [49] N. H. Stair, R. Huang, and F. A. Evangelista, A multireference quantum krylov algorithm for strongly correlated electrons, *Journal of chemical theory and computation* **16**, 2236 (2020).
- [50] C. Kokail, C. Maier, R. van Bijnen, T. Brydges, M. K. Joshi, P. Jurcevic, C. A. Muschik, P. Silvi, R. Blatt, C. F. Roos, *et al.*, Self-verifying variational quantum simulation of lattice models, *Nature* **569**, 355 (2019).
- [51] F. Arute, K. Arya, R. Babbush, D. Bacon, J. C. Bardin, R. Barends, S. Boixo, M. Broughton, B. B. Buckley, *et al.*, Hartree-fock on a superconducting qubit quantum computer, *Science* **369**, 1084 (2020).
- [52] R. Wiersema and N. Killoran, Optimizing quantum circuits with Riemannian gradient flow, *Phys. Rev. A* **107**, 062421 (2023).
- [53] M. Robbiati, E. Pedicillo, A. Pasquale, X. Li, A. Wright, R. M. S. Farias, K. U. Giang, J. Son, J. Knörzer, S. T. Goh, J. Y. Khoo, N. H. Y. Ng, Z. Holmes, S. Carrazza, and M. Gluza, *Double-bracket quantum algorithms for high-fidelity ground state preparation* (2024), [arXiv:2408.03987 \[quant-ph\]](https://arxiv.org/abs/2408.03987).
- [54] L. Xiaoyue, M. Robbiati, A. Pasquale, E. Pedicillo, A. Wright, S. Carrazza, and M. Gluza, Strategies for optimizing double-bracket quantum algorithms, *arXiv preprint arXiv:2408.07431* (2024).
- [55] K. Bharti, A. Cervera-Lierta, T. H. Kyaw, T. Haug, S. Alperin-Lea, A. Anand, M. Degroote, H. Heimonen, J. S. Kottmann, T. Menke, W.-K. Mok, S. Sim, L.-C. Kwek, and A. Aspuru-Guzik, Noisy intermediate-scale quantum algorithms, *Rev. Mod. Phys.* **94**, 015004 (2022).
- [56] M. Cerezo, A. Arrasmith, R. Babbush, S. C. Benjamin, S. Endo, K. Fujii, J. R. McClean, K. Mitarai, X. Yuan, L. Cincio, *et al.*, Variational quantum algorithms, *Nature Reviews Physics* **3**, 625 (2021).
- [57] K. C. Smith, A. Khan, B. K. Clark, S. Girvin, and T.-C. Wei, Constant-depth preparation of matrix product states with adaptive quantum circuits, *PRX Quantum* **5**, 030344 (2024).
- [58] D. Malz, G. Styliaris, Z.-Y. Wei, and J. I. Cirac, Preparation of

- matrix product states with log-depth quantum circuits, *Phys. Rev. Lett.* **132**, 040404 (2024).
- [59] M. Gell-Mann and F. Low, Bound states in quantum field theory, *Phys. Rev.* **84**, 350 (1951).
- [60] M. Larocca, S. Thanasilp, S. Wang, K. Sharma, J. Biamonte, P. J. Coles, L. Cincio, J. R. McClean, Z. Holmes, and M. Cerezo, A review of barren plateaus in variational quantum computing, *arXiv preprint arXiv:2405.00781* (2024).
- [61] M. Cerezo, M. Larocca, D. García-Martín, N. L. Diaz, P. Braccia, E. Fontana, M. S. Rudolph, P. Bermejo, A. Ijaz, S. Thanasilp, *et al.*, Does provable absence of barren plateaus imply classical simulability? or, why we need to rethink variational quantum computing, *arXiv preprint arXiv:2312.09121* (2023).
- [62] A. M. Bloch, Steepest descent, linear programming and Hamiltonian flows, *Contemp. Math. AMS* **114**, 77 (1990).
- [63] J. Moore, R. Mahony, and U. Helmke, Numerical gradient algorithms for eigenvalue and singular value calculations, *SIAM Journal on Matrix Analysis and Applications* **15**, 881 (1994).
- [64] R. Brockett, Dynamical systems that sort lists, diagonalize matrices, and solve linear programming problems, *Linear Algebra and its Applications* **146**, 79 (1991).
- [65] S. T. Smith, *Geometric optimization methods for adaptive filtering* (Harvard University, 1993).
- [66] U. Helmke and J. B. Moore, *Optimization and dynamical systems* (Springer Science & Business Media, 2012).
- [67] A. Bloch, Estimation, principal components and Hamiltonian systems, *Systems & Control Letters* **6**, 103 (1985).
- [68] A. M. Bloch, R. W. Brockett, and T. S. Ratiu, Completely integrable gradient flows, *Communications in Mathematical Physics* **147**, 57 (1992).
- [69] R. Brockett, Least squares matching problems, *Linear Algebra and its Applications* **122-124**, 761 (1989), special Issue on Linear Systems and Control.
- [70] A. M. Bloch, A completely integrable Hamiltonian system associated with line fitting in complex vector spaces, *Bull. Amer. Math. Soc.* DOI: <https://doi.org/10.1090/S0273-0979-1985-15365-0> (1985).
- [71] P. Deift, T. Nanda, and C. Tomei, Ordinary differential equations and the symmetric eigenvalue problem, *SIAM Journal on Numerical Analysis* **20**, 1 (1983).
- [72] M. T. Chu, On the continuous realization of iterative processes, *SIAM Review* **30**, 375 (1988).
- [73] F. Wegner, Flow-equations for hamiltonians, *Annalen der physik* **506**, 77 (1994).
- [74] F. Wegner, Flow equations and normal ordering: a survey, *Journal of Physics A: Mathematical and General* **39**, 8221 (2006).
- [75] M. B. Hastings, On lieb-robinson bounds for the double bracket flow (2022), *arXiv:2201.07141 [quant-ph]*.
- [76] S. D. Glazek and K. G. Wilson, Renormalization of Hamiltonians, *Phys. Rev. D* **48**, 5863 (1993).
- [77] S. D. Glazek and K. G. Wilson, Perturbative renormalization group for Hamiltonians, *Phys. Rev. D* **49**, 4214 (1994).
- [78] S. Kehrein, The flow equation approach to many-particle systems, *Springer Tracts Mod. Phys.* **217**, 1 (2006).
- [79] R. W. Brockett, Smooth dynamical systems which realize arithmetical and logical operations, *Three Decades of Mathematical System Theory: A Collection of Surveys at the Occasion of the 50th Birthday of Jan C. Willems*, 19 (2005).
- [80] E. Malvetti, C. Arenz, G. Dirr, and T. Schulte-Herbrüggen, Randomized gradient descents on riemannian manifolds: Almost sure convergence to global minima in and beyond quantum optimization, *arXiv preprint arXiv:2405.12039* (2024).
- [81] H. Karimi, J. Nutini, and M. Schmidt, Linear convergence of gradient and proximal-gradient methods under the polyak-łojasiewicz condition, in *Machine Learning and Knowledge Discovery in Databases: European Conference, ECML PKDD 2016, Riva del Garda, Italy, September 19-23, 2016, Proceedings, Part I 16* (Springer, 2016) pp. 795–811.
- [82] A. Anshu, D. Gosset, K. J. Morenz Korol, and M. Soleimani-far, Improved Approximation Algorithms for Bounded-Degree Local Hamiltonians, *Phys. Rev. Lett.* **127**, 250502 (2021).
- [83] K. Hejazi, M. Motta, and G. K.-L. Chan, Adiabatic quantum imaginary time evolution, *Phys. Rev. Res.* **6**, 033084 (2024).
- [84] S. Paeckel, T. Köhler, A. Swoboda, S. R. Manmana, U. Schollwöck, and C. Hubig, Time-evolution methods for matrix-product states, *Annals of Physics* **411**, 167998 (2019).
- [85] We thank D. Gosset for pointing out the appearance of the commutator for QITE which he discovered while working on Ref. [82].
- [86] N. A. McMahon, M. Pervez, and C. Arenz, Equating quantum imaginary time evolution, riemannian gradient flows, and stochastic implementations, *arXiv preprint arXiv:2504.06123* (2025).
- [87] C. M. Dawson and M. A. Nielsen, The solovay-kitaev algorithm, *Quantum Information & Computation* **6**, 81 (2006).
- [88] Y.-A. Chen, A. M. Childs, M. Hafezi, Z. Jiang, H. Kim, and Y. Xu, Efficient product formulas for commutators and applications to quantum simulation, *Phys. Rev. Res.* **4**, 013191 (2022).
- [89] A. M. Childs and N. Wiebe, Product formulas for exponentials of commutators, *Journal of Mathematical Physics* **54**, 10.1063/1.4811386 (2013).
- [90] A. M. Childs and R. Kothari, Limitations on the simulation of non-sparse Hamiltonians, *Quantum Information & Computation* **10**, 669 (2010).
- [91] D. W. Berry, A. M. Childs, R. Cleve, R. Kothari, and R. D. Somma, Simulating Hamiltonian Dynamics with a Truncated Taylor Series, *Phys. Rev. Lett.* **114**, 090502 (2015).
- [92] A. M. Childs and N. Wiebe, Hamiltonian simulation using linear combinations of unitary operations, *Quantum Information & Computation* **12**, 901 (2012).
- [93] A. M. Childs, Y. Su, M. C. Tran, N. Wiebe, and S. Zhu, Theory of Trotter Error with Commutator Scaling, *Phys. Rev. X* **11**, 011020 (2021).
- [94] A. M. Childs and Y. Su, Nearly optimal lattice simulation by product formulas, *Phys. Rev. Lett.* **123**, 050503 (2019).
- [95] B. Zindorf and S. Bose, Efficient Implementation of Multi-Controlled Quantum Gates, *arXiv preprint arXiv:2404.02279* (2024).
- [96] S. Balaucă and A. Arusoae, Efficient constructions for simulating multi controlled quantum gates, in *International Conference on Computational Science* (Springer, 2022) pp. 179–194.
- [97] B. Zindorf and S. Bose, Multi-controlled quantum gates in linear nearest neighbor (2025), *arXiv:2506.00695 [quant-ph]*.
- [98] J. L. Bosse and A. Montanaro, Probing ground-state properties of the kagome antiferromagnetic heisenberg model using the variational quantum eigensolver, *Phys. Rev. B* **105**, 094409 (2022).
- [99] J. Kattemölle and J. van Wezel, Variational quantum eigensolver for the heisenberg antiferromagnet on the kagome lattice, *Phys. Rev. B* **106**, 214429 (2022).
- [100] D. Wecker, M. B. Hastings, and M. Troyer, Progress towards practical quantum variational algorithms, *Physical Review A* **92**, 042303 (2015).
- [101] K. Yamamoto, S. Duffield, Y. Kikuchi, and D. Muñoz Ramo, Demonstrating bayesian quantum phase estimation with quan-

- tum error detection, *Phys. Rev. Res.* **6**, 013221 (2024).
- [102] C. R. Clark, H. N. Tinkey, B. C. Sawyer, A. M. Meier, K. A. Burkhardt, C. M. Seck, C. M. Shappert, N. D. Guise, C. E. Volin, S. D. Fallick, H. T. Hayden, W. G. Rellergert, and K. R. Brown, High-fidelity bell-state preparation with $^{40}\text{Ca}^+$ optical qubits, *Phys. Rev. Lett.* **127**, 130505 (2021).
- [103] J. Robledo-Moreno, M. Motta, H. Haas, A. Javadi-Abhari, P. Jurcevic, W. Kirby, S. Martiel, K. Sharma, S. Sharma, T. Shirakawa, I. Sitdikov, R.-Y. Sun, K. J. Sung, M. Takita, M. C. Tran, S. Yunoki, and A. Mezzacapo, Chemistry beyond the scale of exact diagonalization on a quantum-centric supercomputer, *Science Advances* **11**, 10.1126/sciadv.adu9991 (2025).
- [104] R. Seidel, S. Bock, R. Zander, M. Petrić, N. Steinmann, N. Tcholtchev, and M. Hauswirth, Qrisp: A framework for compilable high-level programming of gate-based quantum computers, arXiv preprint arXiv:2406.14792 (2024).
- [105] D. W. Berry, Y. Tong, T. Khattar, A. White, T. I. Kim, G. H. Low, S. Boixo, Z. Ding, L. Lin, S. Lee, G. K.-L. Chan, R. Babbush, and N. C. Rubin, Rapid initial-state preparation for the quantum simulation of strongly correlated molecules, *PRX Quantum* **6**, 020327 (2025).
- [106] D. W. Berry, N. C. Rubin, A. O. Elnabawy, G. Ahlers, A. E. DePrince III, J. Lee, C. Gogolin, and R. Babbush, Quantum simulation of realistic materials in first quantization using non-local pseudopotentials, *npj Quantum Information* **10**, 130 (2024).
- [107] J. Haegeman, J. I. Cirac, T. J. Osborne, I. Pižorn, H. Verschelde, and F. Verstraete, Time-dependent variational principle for quantum lattices, *Phys. Rev. Lett.* **107**, 070601 (2011).
- [108] J. Haegeman, M. Mariën, T. J. Osborne, and F. Verstraete, Geometry of matrix product states: Metric, parallel transport, and curvature, *Journal of Mathematical Physics* **55** (2014).
- [109] L. Vanderstraeten, J. Haegeman, and F. Verstraete, Tangent-space methods for uniform matrix product states, *SciPost Phys. Lect. Notes*, **7** (2019).
- [110] M. Hauru, M. V. Damme, and J. Haegeman, Riemannian optimization of isometric tensor networks, *SciPost Phys.* **10**, 040 (2021).
- [111] B. Vanhecke, M. V. Damme, J. Haegeman, L. Vanderstraeten, and F. Verstraete, Tangent-space methods for truncating uniform MPS, *SciPost Phys. Core* **4**, 004 (2021).
- [112] C. M. Dawson, J. Eisert, and T. J. Osborne, Unifying variational methods for simulating quantum many-body systems, *Phys. Rev. Lett.* **100**, 130501 (2008).
- [113] Q. Miao and T. Barthel, Quantum-classical eigensolver using multiscale entanglement renormalization, *Phys. Rev. Res.* **5**, 033141 (2023).
- [114] J. R. McClean, S. Boixo, V. N. Smelyanskiy, R. Babbush, and H. Neven, Barren plateaus in quantum neural network training landscapes, *Nature Communications* **9**, 1 (2018).
- [115] L. Bittel and M. Kliesch, Training variational quantum algorithms is np-hard, *Phys. Rev. Lett.* **127**, 120502 (2021).
- [116] D. Stilck Franca and R. Garcia-Patron, Limitations of optimization algorithms on noisy quantum devices, *Nature Physics* **17**, 1221 (2021).
- [117] L. Bittel, S. Gharibian, and M. Kliesch, Optimizing the depth of variational quantum algorithms is strongly QCMA-hard to approximate, arXiv preprint arXiv:2211.12519 (2022).
- [118] J. P. LaSalle, The 'bang-bang' principle, *IFAC Proceedings Volumes* **1**, 503 (1960).
- [119] D. Dong and I. R. Petersen, Quantum control theory and applications: a survey, *IET control theory & applications* **4**, 2651 (2010).
- [120] S. Kuang, D. Dong, and I. R. Petersen, Rapid Lyapunov control of finite-dimensional quantum systems, *Automatica* **81**, 164 (2017).
- [121] R. Wang, T. H. Hsieh, and G. Vidal, Bang-bang algorithms for quantum many-body ground states: A tensor network exploration, *Phys. Rev. B* **106**, 195133 (2022).
- [122] P. Caputa, N. Kundu, M. Miyaji, T. Takayanagi, and K. Watanabe, Anti-de Sitter Space from Optimization of Path Integrals in Conformal Field Theories, *Phys. Rev. Lett.* **119**, 071602 (2017).
- [123] J. Boruch, P. Caputa, D. Ge, and T. Takayanagi, Holographic path-integral optimization, *Journal of High Energy Physics* **2021**, 1 (2021).
- [124] R. Dann, A. Tobalina, and R. Kosloff, Fast route to equilibration, *Phys. Rev. A* **101**, 052102 (2020).
- [125] R. Dann, A. Tobalina, and R. Kosloff, Shortcut to equilibration of an open quantum system, *Phys. Rev. Lett.* **122**, 250402 (2019).
- [126] J. Son, M. Gluza, R. Takagi, and N. H. Y. Ng, Quantum dynamic programming, *Phys. Rev. Lett.* **134**, 180602 (2025).
- [127] S. J. Thomson and J. Eisert, Unravelling quantum dynamics using flow equations, *Nature Physics* **20**, 1401 (2024).
- [128] L. Hackl, T. Guaita, T. Shi, J. Haegeman, E. Demler, and J. I. Cirac, Geometry of variational methods: dynamics of closed quantum systems, *SciPost Phys.* **9**, 048 (2020).
- [129] G. Dirr and U. Helmke, Lie theory for quantum control, *GAMM-Mitteilungen* **31**, 59 (2008).
- [130] I. Kurniawan, G. Dirr, and U. Helmke, Controllability aspects of quantum dynamics: a unified approach for closed and open systems, *IEEE transactions on automatic control* **57**, 1984 (2012).
- [131] T. Schulte-Herbrüggen, A. Spörl, N. Khaneja, and S. Glaser, Optimal control for generating quantum gates in open dissipative systems, *Journal of Physics B: Atomic, Molecular and Optical Physics* **44**, 154013 (2011).
- [132] T. Schulte-Herbrüggen, S. Glaser, G. Dirr, and U. Helmke, Gradient flows for optimisation and quantum control: foundations and applications, arXiv preprint arXiv:0802.4195 (2008).
- [133] A. Barenco, C. H. Bennett, R. Cleve, D. P. DiVincenzo, N. Margolus, P. Shor, T. Sleator, J. A. Smolin, and H. Weinfurter, Elementary gates for quantum computation, *Physical Review A* **52**, 3457 (1995).
- [134] S. Lloyd, M. Mohseni, and P. Rebentrost, Quantum principal component analysis, *Nature Physics* **10**, 631 (2014).
- [135] S. Kimmel, C. Y.-Y. Lin, G. H. Low, M. Ozols, and T. J. Yoder, Hamiltonian simulation with optimal sample complexity, *npj Quantum Inf.* **3**, 13 (2017).
- [136] M. Kjaergaard, M. Schwartz, A. Greene, G. Samach, A. Bengtsson, M. O'Keeffe, C. McNally, J. Braumüller, D. Kim, P. Krantz, *et al.*, Demonstration of density matrix exponentiation using a superconducting quantum processor, *Physical Review X* **12**, 011005 (2022).
- [137] M. B. Hastings, Entropy and entanglement in quantum ground states, *Phys. Rev. B* **76**, 035114 (2007).
- [138] R. Bhatia, *Matrix analysis*, Vol. 169 (Springer Science & Business Media, 1996).
- [139] V. Lotfi and S. Sarin, A graph coloring algorithm for large scale scheduling problems, *Computers & Operations Research* **13**, 27 (1986).
- [140] G. Song and A. Klappenecker, The simplified toffoli gate implementation by margolus is optimal (2003), arXiv:quant-ph/0312225 [quant-ph].
- [141] C. Gidney, Halving the cost of quantum addition, *Quantum* **2**, 74 (2018).

- [142] T. Khattar and C. Gidney, [Rise of conditionally clean ancillae for optimizing quantum circuits](#) (2024), [arXiv:2407.17966 \[quant-ph\]](#).
- [143] G. Li, Y. Ding, and Y. Xie, Tackling the qubit mapping problem for nisq-era quantum devices, in *Proceedings of the twenty-fourth international conference on architectural support for programming languages and operating systems* (2019) pp. 1001–1014.
- [144] T. Yamamoto and R. Ohira, Error suppression by a virtual two-qubit gate, *Journal of Applied Physics* **133** (2023).
- [145] S. Efthymiou, A. Orgaz-Fuertes, R. Carobene, J. Cereijo, A. Pasquale, S. Ramos-Calderer, S. Bordoni, D. Fuentes-Ruiz, A. Candido, E. Pedicillo, M. Robbiati, Y. P. Tan, J. Wilkens, I. Roth, J. I. Latorre, and S. Carrazza, Qibolab: an open-source hybrid quantum operating system, *Quantum* **8**, 1247 (2024).

End Matter

Geometry of ITE DBF. — We show that the ITE dynamics in Eq. (5) represents the minimization of a cost function using its steepest gradient on the Riemannian manifold. To this end, we first show the fundamentals of DBFs and then elaborate on the property of ITE in terms of DBFs.

In general, DBFs are matrix-valued ordinary differential equations which have been shown to realize diagonalization, QR decompositions, sorting and other tasks [64, 66, 71, 72]. Brockett first introduced the flow equation by studying the minimization of the least square of two matrices with the steepest descent techniques. Let $\mathcal{M}(A) = \{UAU^\dagger \text{ s.t. } U^{-1} = U^\dagger\}$ be the set of all matrices generated by evolving a Hermitian operator A under a unitary U . Consider the loss $\mathcal{L}_{A,B}(U) = -\frac{1}{2}\|UAU^\dagger - B\|_{\text{HS}}^2$ where B is also Hermitian. Then, the Riemannian gradient evaluated at $P = UAU^\dagger$ for the loss function $\mathcal{L}_B(P) = -\frac{1}{2}\|P - B\|_{\text{HS}}^2$ is given by [52, 66]

$$\text{grad}_P \mathcal{L}_B(P) = [[P, B], P]. \quad (17)$$

We note that the derivation relies on two conditions of Riemannian geometry, namely, the tangency condition and the compatibility condition, see Refs. [52, 66] for a derivation.

This indicates that the the right-hand side of Eq. (17) is indeed the steepest descent direction of the cost function on the Riemannian manifold $\mathcal{M}(A)$. As the steepest-descent flow is the set of points $A(\ell) \in \mathcal{M}(A)$ which satisfy

$$\partial A(t)/\partial t = \text{grad}_{A(t)} \mathcal{L}_B(A(t)), \quad (18)$$

we arrive at the flow equation

$$\partial A(t)/\partial t = [[A(t), B], A(t)], \quad (19)$$

which is exactly the DBF.

In case of the ground-state preparation task, we obtain the ITE in Eq. (5) by setting $A = \Psi(\tau) = |\Psi(\tau)\rangle\langle\Psi(\tau)|$ and $B = \hat{H}$. Namely, the ITE realizes the minimization of the cost function

$$\mathcal{L}_{\hat{H}}(\Psi(\tau)) = -\frac{1}{2}\|\Psi(\tau) - \hat{H}\|_{\text{HS}}^2, \quad (20)$$

using its steepest descent direction on the Riemannian manifold. Eq. (20) can be simplified to

$$\mathcal{L}_{\hat{H}}(\Psi(\tau)) = E(\tau) - \frac{1}{2}(1 + \|\hat{H}\|_{\text{HS}}^2). \quad (21)$$

As the second term is independent of τ , we can clearly verify that the cost function considered in this task is equivalent to the minimization of the energy, i.e., the preparation of the ground-state. Combining this observation with Eq. (19) we obtain Eq. 5. That is, we see that DBFs provide a solution to ITE, as claimed. We remark that the ITE and Brockett’s DBF have been extensively studied in slightly different fields, but their link has not been pointed out to the best of our knowledge. However, individually they have been linked to gradient flows, see Ref. [128] for a discussion of ITE as gradient flow and Refs. [62, 63, 65, 129–132] for a discussion of DBFs in context of gradient flows.

We also demonstrate some properties of QITE that can be inferred through the lens of DBF. For instance, the convergence to the ground-state can be checked by utilizing the properties of the DBF flow. The solution of the DBF in Eq. (19) is known to converge to the equilibria point that is characterized by $[A(\infty), B] = 0$; that is, $A(\infty)$ shares the same eigenbasis with B . Also, the DBF has the isospectral property, meaning any solution of the DBF has the same set of eigenvalues. In case of the setting in Eq. (20), as the initial state $\Psi(0)$ is pure (i.e., a rank-one matrix) and the cost function in Eq. (21) indicates the energy minimization, the solution always converges to only one non-trivial eigenstate, i.e., the ground-state.

One can also derive the energy-fluctuation refrigeration relation for ITE in Eq. (3) directly from the link with DBFs. Concretely, by taking the derivative of Eq. (1), we can see that the energy of ITE is driven by the energy fluctuation. As for the DBF, the derivative of the cost function in Eq. (20) reads

$$\partial \mathcal{L}_{\hat{H}}(\Psi(\tau))/\partial \tau = -\|[\Psi(\tau), \hat{H}]\|_{\text{HS}} \quad (22)$$

and further calculation reveals that

$$\|[\Psi(\tau), \hat{H}]\|_{\text{HS}} = 2V(\tau). \quad (23)$$

This indicates that the energy dynamics of both cases are the same. See [II B](#) of Supplemental Materials for more discussion.

Circuit depths for iterative applications of DB-QITE.— Theorem 2 ensures that the fidelity with the ground-state converges exponentially with the number of DBQA steps k . However, the depth of circuit (i.e., the number of queries to the Hamiltonian simulation, to reflections around the reference state or to initial state preparation circuit) also scales exponentially in k . Specifically, Eq. (13) reveals that k steps of DB-QITE require $\mathcal{O}(3^k)$ subroutine queries to Hamiltonian simulation or partial reflections around the reference state.

The reflection unitary is a multi-qubit controlled parameterized phase gate, assuming the quantum state is the tensor-product zero state. Multi-qubit controlled gates can be implemented efficiently without qubit overheads [133]. Indeed Theorem 1 of Ref. [95] proves that any multi-qubit controlled unitary gate with $m \geq 6$ controls is realizable by $12L - 32$

CNOT gates with depth $8L - 8$, $16L - 48$ T gates with depth $8L - 6$ and $8L - 32$ Hadamard gates with depth $4L - 11$. The App. V describes the implementation in Qrisp which uses additional insights to further reduce these scalings. This suggests that the gate complexity is linear in the number of qubits which is similar to efficient Hamiltonian simulation compiling [90–94].

Given the exponential query complexity in k , the DB-QITE analyzed in Theorem 2 amplifies the initial fidelity F_0 to a prescribed final fidelity F_{th} in depth

$$\mathcal{O}(L) \times \mathcal{O}\left(\left(\frac{1 - F_0}{1 - F_{\text{th}}}\right)^{24\|\hat{H}\|^3/(F_0\Delta^2)}\right), \quad (24)$$

where we multiplied the depth upper bound of the subroutines $\mathcal{O}(L)$ by the exponential query complexity, see Sec. IV for derivation. Thus, the depth scales exponentially with the inverse spectral gap Δ and with the inverse of the initial ground-state fidelity F_0 . The base of the exponential scaling is the ratio of the initial and final infidelity. The last factor in the exponent is the inverse dependence on the step duration given in Eq. (15). For local Hamiltonians this step duration is polynomially decreasing in the number of qubits L implying that the runtime grows exponentially with L^3 . Thus, the DB-QITE scheduling involved in the rigorous analysis allows for only a small number of steps k so that circuit depths are modest.

There are strong indications that this runtime analysis is unnecessarily pessimistic. In order to prove the Theorem we needed to use bounds that facilitated multiplicative rather than additive relations between the infidelities of consecutive DB-QITE states. This is rather intricate and the bounds can be expected to not be tight. More specifically, Eq. (15) arises from taking a coarse lower bound $E_k \geq \Delta(1 - F_k)$ which relates the energy to the fidelity F_k . This lower bound is saturated if the k 'th DB-QITE state $|\omega_k\rangle$ is supported only on the the ground-state $|\lambda_0\rangle$ and the first excited state $|\lambda_1\rangle$. For such superposition of the two unknown lowest eigenstates, we can replace the Hamiltonian in our analysis by $\hat{H}_{\text{eff}} = \Delta|\lambda_1\rangle\langle\lambda_1|$. If \hat{H} is gapped then the scheduling Eq. (15) would be independent of the system size and the runtime would be system-size independent.

In turn, when the bound is not saturated then knowledge of E_k (which is a basic measurement for monitoring any ground-state preparation quantum algorithm) would allow to choose a longer step duration and hence gain a larger energy decrease [32, 54]. For an unconstrained step duration s_k in Eq. (12) an intermediate relation in the proof states

$$F_{k+1} = F_k + 2E_k s_k + \mathcal{O}(s_k^2). \quad (25)$$

The magnitude of the higher-order terms determines the maximal step duration s_k . Rather than taking worst case estimates as we had to do in the proof, the higher-order terms can be estimated from simple measurements of the energy E_k as a function of s_k in Eq. (12), see Ref. [54] for numerical examples. In the proof, we upper bound the higher-order terms by the norm of the Hamiltonian but this is very likely a big over-estimate. Indeed, those upper bounds are saturated when $|\omega_k\rangle$ is a superposition of the lowest and highest eigestates, which is highly

unlikely. Indeed, there is strong numerical evidence that in practice rather long steps can be used [32, 40, 53, 54, 127]. This makes it plausible that DB-QITE can be scheduled to gain much more fidelity in every step than is guaranteed by the worst-case lower bound Eq. (16) which implies a much shorter circuit depth in those cases.

Comparison with prior work.—Ref. [82] proposed circuit synthesis which provides an energy gain over product states in amount decided by energy fluctuations. This is similar to Eq. (14) so we can reinterpret the energy reduction in Ref. [82] as being close to steepest-descent flows. Ref. [82] improves the energy only for product states and hence cannot be iterated. In contrast, Thms. 1 and 2 apply to arbitrary state initializations. Thus we not only amplify energy reductions with similarly short depth circuits as Ref. [82], but also allow the energy of arbitrary initial states to be reduced which allows to iterate our circuit synthesis. By this, the recursive character of DB-QITE should be viewed as a bonus despite the overheads associated with circuit repetitions.

Ref. [52] also exploits the commutator form of Riemannian gradients and derived a method for optimizing quantum circuits. Their proposal aims to implement Eq. (8) by learning from measurements the parameters of the unitary. The protocol has rigorous convergence guarantees only in the limit of performing an exponential number of measurements and could be prohibitively expensive.

Quantum dynamic programming.— Let us comment how to reduce the circuit depth by extending its width. Any state $|\psi\rangle = U_\psi|0\rangle$ can be improved into a state with lowered energy by setting $|\psi'\rangle = U^{(\psi)}|\psi\rangle$ where

$$U^{(\psi)} = e^{i\sqrt{\tau}\hat{H}} e^{i\sqrt{\tau}|\psi\rangle\langle\psi|} e^{-i\sqrt{\tau}\hat{H}}. \quad (26)$$

Thus in each step, DB-QITE depends on the input state's density matrix in a non-trivial way and so it is a quantum recursion. Recently, quantum dynamic programming has been proposed [126] which similarly to ordinary dynamic programming leverages memoization to reduce the runtime of recursions. In this case it suffices to combine density matrix exponentiation for the reflector $e^{i\sqrt{\tau}|\psi\rangle\langle\psi|}$ with regular Hamiltonian simulation. See. [20, 23] for discussion how to perform QITE using qubitization.

The reflection operator can be implemented using the density matrix exponentiation of $|0\rangle\langle 0|$. Here, the cost scalings of the circuit depth and the number of copies of quantum states are respectively $\mathcal{O}(n\theta^2/\epsilon)$ and $\mathcal{O}(\theta^2/\epsilon)$ for implementing $e^{-i\theta\rho}$ [134, 135]. While the precise realization could be costly, performing density-matrix exponentiation also seems feasible because the $|0\rangle$ is known and so each time a copy is needed it can be prepared through a reset operation [136].

We stress that $U^{(\psi)}$ can be implemented obliviously to the circuit that prepares $|\psi\rangle$. Thus, DB-QITE implemented through dynamic programming could be viewed a *distillation* protocol of states with lowered energy. The inverse of the number of quantum states needed to implement one step of density matrix exponentiation is a lower bound to the rate of approximate distillation. If we want the distillation to have an increased gain we can perform more steps but with the trade-off that the rate will decay exponentially.

Supplemental Material for “Double-bracket quantum algorithms for quantum imaginary-time evolution”

Marek Gluza,^{1,*} Jeongrak Son,¹ Bi Hong Tiang,¹ René Zander,²
Raphael Seidel,² Yudai Suzuki,^{3,4} Zoë Holmes,³ and Nelly H. Y. Ng^{1,5,†}

¹*School of Physical and Mathematical Sciences, Nanyang Technological University, 637371, Singapore*

²*Fraunhofer Institute FOKUS, Berlin, Germany*

³*Institute of Physics, Ecole Polytechnique Fédérale de Lausanne (EPFL), Lausanne, Switzerland*

⁴*Quantum Computing Center, Keio University, Hi-yoshi 3-14-1, Kohoku-ku, Yokohama 223-8522, Japan*

⁵*Centre for Quantum Technologies, National University of Singapore, 3 Science Drive 2, 117543, Singapore*

(Dated: July 3, 2025)

Contents

References	5
I. Common terminology and techniques	12
II. Key properties of imaginary-time evolution (ITE)	13
A. Proof that imaginary-time evolution is a solution to a double-bracket flow	13
B. Fluctuation-refrigeration relation for the ITE cooling rate	14
C. Digression: Exponential convergence of thermal states to ground-states in 1-norm	15
D. Exponential convergence of fidelity to the ground-state through ITE	16
III. Double-bracket iteration (DBI) approach to QITE	16
A. Useful lemmas for proving fluctuation-refrigeration relation and fidelity convergence of QITE DBI	17
B. Proof of fluctuation-refrigeration relation for QITE DBI and its cooling rate	18
C. Exponential fidelity convergence of QITE DBI	20
IV. Double-Bracket Quantum Imaginary-Time Evolution (DB-QITE)	22
A. Fluctuation-refrigeration relation of DB-QITE	23
B. Exponential fidelity convergence of DB-QITE: Proof of Theorem 2	25
C. Runtime consideration	29
V. Numerical simulations and gate-counts of DB-QITE using Qrisp	29
A. Compilation for DB-QITE	29
B. Numerical simulations of the Heisenberg model and initial states	30
C. Conditions for quantum phase estimation (QPE) to outperform DB-QITE	34

* marekludwik.gluza@ntu.edu.sg

† nelly.ng@ntu.edu.sg

I. Common terminology and techniques

In this section, we make a comprehensive list of common terminology used throughout the rest of the appendix.

1. The *Hilbert-Schmidt norm* (or *Frobenius norm*) of an operator A acting on a Hilbert space \mathcal{H} is defined as:

$$\|A - B\|_{\text{HS}} = \sqrt{\text{Tr}((A - B)^\dagger (A - B))}. \quad (27)$$

2. The *operator norm* $\|\hat{X}\|$ is defined as the smallest number such that for all normalized vectors, $\|\hat{X}\psi\| \leq \|\hat{X}\|$ holds:

$$\|\hat{X}\| = \sup_{\|\psi\|=1} \|\hat{X}\psi\|. \quad (28)$$

When the operator \hat{X} is Hermitian on a finite-dimensional inner product space, its operator norm is equal to the maximum absolute value of its eigenvalues. Any norm satisfies the *triangle inequality* $\|x + y\| \leq \|x\| + \|y\|$.

3. The Taylor series expansion of a function $f(x)$ around x_0 , truncated at the n -th term, is

$$f(x) = f(x_0) + f^{(1)}(x_0)(x - x_0) + \cdots + \frac{f^{(n-1)}(x_0)}{(n-1)!}(x - x_0)^{n-1} + \frac{1}{n!}(x - x_0)^n f^{(n)}(\xi). \quad (29)$$

where $f^{(n+1)}(t)$ is the $(n+1)$ -th derivative of f and $\xi \in [x_0, x]$.

4. For two pure quantum states $|\psi\rangle$ and $|\Omega\rangle$, the fidelity is defined as $F(|\psi\rangle, |\Omega\rangle) = |\langle\psi|\Omega\rangle|^2$. To analyze fidelity convergence in QITE, it is useful to derive bounds on the expected energy and energy variance in terms of the ground-state infidelity, $\epsilon = 1 - F$ and the spectrum of eigenenergies $\{\lambda_j\}_j$.

Lemma 3. Let $|\Omega\rangle$ be any pure state. Denote Hamiltonian as $\hat{H} = \sum_{j=0}^{d-1} \lambda_j |\lambda_j\rangle\langle\lambda_j|$ where we assume that the eigenvalues of \hat{H} are ordered increasingly and we set $\lambda_0 = 0$. Suppose that the ground-state fidelity is given by $F = 1 - \epsilon$, then we have

$$E_k \geq \lambda_1 \epsilon, \quad \text{and} \quad V_k \leq \lambda_{d-1}^2 \epsilon, \quad (30)$$

where $E_k = \langle\Omega|\hat{H}^2|\Omega\rangle$ is the expected energy and $V_k = \langle\Omega|\hat{H}^2|\Omega\rangle - E_k^2$ is the energy variance.

Proof. Let's define the probability to occupy the i -th eigenstate $|\lambda_i\rangle$ as p_i . As the ground-state fidelity is given by $F = 1 - \epsilon$, the state has probability $p_0 = 1 - \epsilon$ to occupy the ground-state. Since $\lambda_0 = 0$ by assumption, we obtain

$$E_k = \sum_{i=1}^{d-1} \lambda_i p_i \geq \lambda_1 \sum_{i=1}^{d-1} p_i = \lambda_1 \epsilon, \quad \text{and} \quad V_k \leq \sum_{i=1}^{d-1} \lambda_i^2 p_i \leq \|\hat{H}\|^2 \sum_{i=1}^{d-1} p_i = \|\hat{H}\|^2 \epsilon_k. \quad (31)$$

□

	Sec. (II): ITE	Sec. (III): QITE DBI	Sec. (IV): DB-QITE
Initial state	$ \Psi_0\rangle$	$ \sigma_0\rangle = \Psi_0\rangle$	$ \omega_0\rangle = \Psi_0\rangle$
Evolution time step	Continuous duration τ	Discrete duration s_k	Discrete duration s_k
Evolved states	$ \Psi(\tau)\rangle$, see Eq. (32)	$ \sigma_k\rangle$, see Eq. (59)	$ \omega_k\rangle$, see Eq. (124)
Expected energy	$E(\tau) = \langle\Psi(\tau) \hat{H} \Psi(\tau)\rangle$	$\bar{E}_k = \langle\sigma_k \hat{H} \sigma_k\rangle$	$E_k = \langle\omega_k \hat{H} \omega_k\rangle$
Energy variance	$V(\tau) = \langle\Psi(\tau) \hat{H}^2 \Psi(\tau)\rangle - E(\tau)^2$	$\bar{V}_k = \langle\sigma_k \hat{H}^2 \sigma_k\rangle - \bar{E}_k^2$	$V_k = \langle\omega_k \hat{H}^2 \omega_k\rangle - E_k^2$
Fluctuation-refrigeration relation	$\partial_\tau E(\tau) = -2V(\tau)$	$\bar{E}_{k+1} \leq \bar{E}_k - 2s_k \bar{V}_k + \mathcal{O}(s_k^2)$	$\bar{E}_{k+1} \leq \bar{E}_k - 2s_k V_k + \mathcal{O}(s_k^2)$
Time step conditions for $E_{k+1} - E_k \leq -s_k V_k$	N.A.	$s_k \leq \frac{\bar{V}_k}{4\ \hat{H}\ \langle\sigma_k \hat{H}^2 \sigma_k\rangle}$ (Proposition 11)	$s_k \leq \frac{4V_k}{5\epsilon_k\ \hat{H}\ ^4}$ (Theorem 16)
ground-state fidelity	$F(\Psi(\tau)\rangle, \lambda_0\rangle) = \langle\lambda_0 \Psi(\tau)\rangle ^2$	$F_k = \langle\lambda_0 \sigma_k\rangle ^2 = 1 - \epsilon_k$	$F_k = \langle\lambda_0 \omega_k\rangle ^2 = 1 - \epsilon_k$
ground-state fidelity convergence	$F(\Psi(\tau)\rangle, \lambda_0\rangle) \geq 1 - \delta_H$	$F_k \geq 1 - q^k$ with $q = 1 - sF_0\lambda_1$	$F_k \geq 1 - q^k$ with $q = 1 - sF_0\Delta$
Time step conditions for the above fidelity convergence	$\tau_H = \log \left[O \left(\frac{L}{\delta_H \langle\lambda_0 \Psi_0\rangle ^2} \right) \right]$ (Sec. IID)	$s = \frac{\sqrt{F_0}}{4\ \hat{H}\ }$ (Theorem 13)	$s = \frac{\Delta}{12\ \hat{H}\ ^3}$ (Theorem (2) of main text and Sec. IV B)

TABLE II. The summary of notations for imaginary-time evolution (ITE), quantum imaginary-time evolution with double-bracket flows (QITE DBI), and with the explicit compilation using techniques in double-bracket quantum algorithms (DB-QITE), for ease of reference. For all sections of the supplemental materials, we define the Hamiltonian as $\hat{H} = \sum_{j=1}^{d-1} \lambda_j |\lambda_j\rangle\langle\lambda_j|$ where d is the dimension of the Hamiltonian. We also denote the spectral gap as $\Delta = \lambda_1 - \lambda_0$ where λ_1 and λ_0 represent the first excited and ground-state energy respectively. We also define $\|\hat{H}\|$ as the operator norm of the Hamiltonian. Finally, we assume that the initial state has some non-zero ground-state overlap $F_0 > 0$.

II. Key properties of imaginary-time evolution (ITE)

This is a section that outlines all the key properties of ITE which are relevant for the scope of our work. We begin with the key observation in Section II A that the state defined via ITE is a solution to the double-bracket flow equation. This leads to the decrease in average energy of the ITE state with respect to time, indicating convergence towards the ground-state. In Section II B, we derive a fluctuation-refrigeration relation which shows that states with higher energy fluctuations have a higher cooling rate. We next provide a digression in Section II C discussing convergence of thermal states to ground-states. We then carry over the techniques used in this section, to present in Section II D an exponential convergence of the ITE state's fidelity to the ground-state. This means that implementation of ITE DBF Eq. (33) as a double-bracket quantum algorithm [32] will converge to the ground-state too.

A. Proof that imaginary-time evolution is a solution to a double-bracket flow

Recall the definition for $\tau > 0$, and an initial pure state vector $|\Psi_0\rangle$ we set

$$|\Psi(\tau)\rangle = \frac{e^{-\tau\hat{H}}|\Psi_0\rangle}{\|e^{-\tau\hat{H}}|\Psi_0\rangle\|}, \quad (32)$$

where $\|\psi\| = \sqrt{\langle\psi|\psi\rangle}$ for any vector $|\psi\rangle$. Next, we prove a key connection between ITE and DBFs.

Proposition 4 (ITE is a solution to a DBF). *The ITE pure state $\hat{\Psi}(\tau) = |\Psi(\tau)\rangle\langle\Psi(\tau)|$ is a unique solution to Brockett's double-bracket flow equation, i.e.*

$$\frac{\partial\Psi(\tau)}{\partial\tau} = [[\Psi(\tau), \hat{H}], \Psi(\tau)]. \quad (33)$$

We refer to Eq. (33) as ITE DBF.

Proof. First, observe that the ITE map Eq. (1) is smooth as a function of τ . Second, ITE preserves the state vector normalisation so there must exist a unitary U_τ that implements it. Smoothness implies that there is a unique unitary U_τ such that $|\Psi(\tau)\rangle = U_\tau|\Psi_0\rangle$. We begin the proof by denoting the normalization factor of ITE as

$$N(\tau) = \|e^{-\tau\hat{H}}|\Psi_0\rangle\| = \sqrt{\langle\Psi_0|e^{-2\tau\hat{H}}|\Psi_0\rangle},$$

and evaluating its derivative to be

$$\partial_\tau(N(\tau)) = \frac{-\langle\Psi_0|\hat{H}e^{-2\tau\hat{H}}|\Psi_0\rangle}{N(\tau)}. \quad (34)$$

Thus the change of the ITE state vector as a function of τ is [59]

$$\partial_\tau|\Psi(\tau)\rangle = \partial_\tau\left(\frac{e^{-\tau\hat{H}}|\Psi_0\rangle}{N(\tau)}\right) = \frac{-\hat{H}e^{-\tau\hat{H}}|\Psi_0\rangle}{N(\tau)} + \frac{e^{-\tau\hat{H}}|\Psi_0\rangle \cdot (-\partial_\tau N(\tau))}{N(\tau)^2} \quad (35)$$

$$= -\hat{H}|\Psi(\tau)\rangle + \frac{\langle\Psi_0|\hat{H}e^{-2\tau\hat{H}}|\Psi_0\rangle}{N(\tau)^2}|\Psi(\tau)\rangle \quad (36)$$

$$= -\hat{H}|\Psi(\tau)\rangle + \langle\Psi(\tau)|\hat{H}|\Psi(\tau)\rangle|\Psi(\tau)\rangle. \quad (37)$$

As a remark, this is of the form of a nonlinear Schrödinger equation. On the other hand, we note that the ITE density matrix also satisfies $\Psi(\tau) = |\Psi(\tau)\rangle\langle\Psi(\tau)| \equiv U_\tau\Psi_0U_\tau^\dagger$ satisfies

$$[\Psi(\tau), \hat{H}]|\Psi(\tau)\rangle = |\Psi(\tau)\rangle\langle\Psi(\tau)|\hat{H}|\Psi(\tau)\rangle - \hat{H}|\Psi(\tau)\rangle\langle\Psi(\tau)|\Psi(\tau)\rangle = -\hat{H}|\Psi(\tau)\rangle + E(\tau)|\Psi(\tau)\rangle. \quad (38)$$

Thus, from Eq. (37) we have $\partial_\tau|\Psi(\tau)\rangle = [\Psi(\tau), \hat{H}]|\Psi(\tau)\rangle$. To complete the proof we set $\mathcal{W} = i[\Psi(\tau), \hat{H}]$ and obtain Eq. (5) as the von Neumann evolution equation of the ITE density matrix. \square

Remark. Note that Eq. (5) is a Brockett DBF, see discussion in End Matter. Let us discuss the physical meaning of this ITE state. First, the expected energy of $\Psi(\tau)$ will keep decreasing until it reaches some fixed point Ψ_∞ . Clearly, the condition for a fixed point is $[\Psi_\infty, \hat{H}] = 0$, i.e. both of them are diagonalizable in the energy basis. Thus, they can be expressed as

$$\hat{H} = \sum_{j=1}^{d-1} \lambda_j |\lambda_j\rangle\langle\lambda_j| \quad \text{and} \quad |\Psi(\infty)\rangle = \sum_{j=0}^{d-1} c_j |\lambda_j\rangle\langle\lambda_j|. \quad (39)$$

Without loss of generality, we assume that the eigenvalues of \hat{H} are ordered increasingly, i.e. $\lambda_n \leq \lambda_{n+1}$. Note that $\Psi(\tau)$ is a pure state, and any unitary conjugation preserves rank. Additionally, since Ψ_∞ is diagonalizable in the energy basis, this means that it is an energy eigenstate. This means that for values of $\tau > 0$, the ITE state converges to the ground-state $\Psi_\infty = |\lambda_0\rangle\langle\lambda_0|$. On the other hand, if $\tau < 0$, then the ITE state converges to $\Psi_\infty = |\lambda_{d-1}\rangle\langle\lambda_{d-1}|$ which is the highest energy state of \hat{H} .

B. Fluctuation-refrigeration relation for the ITE cooling rate

In this section, our aim is to derive a *fluctuation-refrigeration relation* for DBF, which shows that states with high energy fluctuation will converge to the ground-state more quickly by ITE procedure. We have seen that in the continuous-time DBF formalism, the average energy in the ITE state vector should decrease when τ increases as it converges to the ground-state, i.e.

$$E(\tau) := \langle\Psi(\tau)|\hat{H}|\Psi(\tau)\rangle \quad (40)$$

is a decreasing function of τ . We show that the decrease rate is dictated by the energy variance $V(\tau) := \langle\Psi(\tau)|\hat{H}^2|\Psi(\tau)\rangle - E(\tau)^2$.

Proposition 5 (ITE Fluctuation-refrigeration relation). *The derivative of average energy with respect to inverse temperature, $\partial_\tau E(\tau)$, is given by*

$$\partial_\tau E(\tau) = -2V(\tau). \quad (41)$$

Proof. We may evaluate the derivative directly using Eq. (37) and the Leibniz chain rule,

$$\partial_\tau E(\tau) = \langle \Psi(\tau) | (E(\tau) - \hat{H}) \hat{H} | \Psi(\tau) \rangle + \langle \Psi(\tau) | \hat{H} (E(\tau) - \hat{H}) | \Psi(\tau) \rangle. \quad (42)$$

Combining the two terms give $\partial_\tau E(\tau) = -2\langle \Psi(\tau) | \hat{H}^2 | \Psi(\tau) \rangle + 2E(\tau)\langle \Psi(\tau) | \hat{H} | \Psi(\tau) \rangle = -2V(\tau)$. \square

Remark. To understand the limits of the relation let us look at asymptotic upper bounds. We will find that they can be attained for ‘hot’ states, where energy fluctuations scale in the system size. On the other hand, for states close to eigenstates energy fluctuations vanish. For a general quantum system, the energy fluctuation is upper bounded by

$$V(\tau) \leq \langle \Psi(\tau) | \hat{H}^2 | \Psi(\tau) \rangle \leq \|\hat{H}\|^2. \quad (43)$$

A stronger bound is obtained for local Hamiltonians, e.g. if they involve I terms $\hat{H} = \sum_{i=1}^I \hat{H}_i$ where each $\|\hat{H}_i\| \leq \mathcal{O}(1)$ has norm independent of system size. In this case, for a system containing L qubits,

$$E(\tau) \leq \mathcal{O}(L), \quad V(\tau) \leq \mathcal{O}(L^2). \quad (44)$$

For example for the transverse field Ising model $\hat{H}_{\text{TIFIM}} = \sum_{i=1}^{L-1} (Z_i Z_{i+1} + X_i)$ we can set $\hat{H}_i = Z_i Z_{i+1} + X_i$ where Z_i and X_i act on qubit i and we have $\|\hat{H}_i\| = 2$. For $|\Psi_0\rangle = |+\rangle^{\otimes L}$ we have $E(0) = L - 1$ and $V(0) = L - 1$ because $(Z_i Z_{i+1})^2 = 1$ and contribute to the energy fluctuation.

C. Digression: Exponential convergence of thermal states to ground-states in 1-norm

We will next recall a result by Hastings [137] who showed that thermal states of gapped Hamiltonians converge exponentially fast to the ground-state if it is unique and the density of eigenstates above the gap is polynomial. This is a digression because in our work we are dealing with pure states rather than thermal states which are generically mixed. However, the discussion is instructive because the same assumption and same mathematical idea will allow us to show an analogous result for ITE.

More specifically, in Ref. [137], Hastings identified a condition on the density of states which suffices to obtain the scaling of the inverse temperature of a thermal state such that it approximates the unique ground-state of a gapped system. More specifically, let \hat{H} be a Hamiltonian with eigenvalues $\{\lambda_j\}$ and we have labeled by $j = 0, 1, \dots, \dim(\hat{H}) - 1$, again ordering the eigenvalues increasingly such that $\lambda_j \leq \lambda_{j+1}$. Furthermore, let us set the ground-state energy as $\lambda_0 = 0$. We can define a simple counting function that captures the density of energy eigenstates. In particular, given the spectral gap $\Delta = \lambda_1 - \lambda_0$, let us define a series of intervals $\mathcal{M}_m := [m\Delta, (m+1)\Delta)$. The function $\rho_m(\hat{H}) = |\{\lambda_j \in \mathcal{M}_m\}|$, for $m = 0, 1, 2, \dots$ therefore counts the number of eigenvalues in each interval \mathcal{M}_m . With this definition, Hastings’ polynomial density of states condition is expressed as

$$\rho_m(\hat{H}) \leq (c_H L)^m / m! \quad (45)$$

for $c_H = \mathcal{O}(1)$, L being the number of qubits. In other words, we assume that the distribution of eigenenergies is sparse near the ground-state for any gapped Hamiltonian. This allows to bound for any inverse temperature β the partition function

$$Z_\beta = \sum_{j=0}^{\dim(\hat{H})-1} e^{-\beta\lambda_j} \leq e^{-\beta\lambda_0} \left[\sum_{m=0}^{\infty} \rho_m(\hat{H}) e^{-\beta\Delta m} \right] \leq e^{-\beta\lambda_0} \sum_{m=0}^{\infty} \frac{(e^{-\beta\Delta} c_H L)^m}{m!} \quad (46)$$

$$= e^{-\beta\lambda_0} \exp(e^{-\beta\Delta} c_H L) \quad (47)$$

where in the first inequality, we use the fact that for all $\lambda_j \in \mathcal{M}_m$, we have that $\lambda_j \geq m\Delta$ and therefore $e^{-\beta\lambda_j} \leq e^{-\beta\Delta m}$. To illustrate this further, if $\rho_0 = |\lambda_0\rangle\langle\lambda_0|$ is the ground-state projector and $\rho^{(\beta)} = \exp(-\beta\hat{H})/Z_\beta$ is the thermal state (as opposed to ITE state it is generically mixed and not pure), then

$$\|\rho^{(\beta)} - \rho_0\| \leq 2 \sum_{m=1}^{\infty} \rho_m(\hat{H}) e^{-\beta\Delta m} \leq 2 [\exp(e^{-\beta\Delta} c_H L) - 1]. \quad (48)$$

Thus, if we set

$$\beta_H = \frac{1}{\Delta} \left[\log \left(\frac{c_H L}{\log(1 + \varepsilon/2)} \right) \right], \quad (49)$$

then $\|\rho^{(\beta_H)} - \rho_0\| \leq \varepsilon$. To understand this more intuitively we use $\log(1 + \varepsilon/2) \geq \varepsilon/4$ which implies $\beta_H \leq \frac{1}{\Delta} \log(\mathcal{O}(L\varepsilon^{-1}))$. This means that thermal states of gapped Hamiltonians converge to the respective ground-states in inverse temperature scaling logarithmically in the system size and the desired approximation precision.

D. Exponential convergence of fidelity to the ground-state through ITE

In the previous section, we studied the exponential convergence of thermal states to the ground-state, under Hastings' condition on the system Hamiltonian. However, the central interest of this work revolves around ITE states. While such states are pure as opposed to generically mixed thermal states, both involve an imaginary-time exponential of the Hamiltonian and a normalization. This is a key feature that allows for similar fidelity convergence behavior on the ITE state, to the ground-state.

To see this explicitly, we apply a similar consideration to the ground-state fidelity of the ITE which we define as

$$F(|\Psi(\tau)\rangle, |\lambda_0\rangle) = |\langle\lambda_0|\Psi(\tau)\rangle|^2 = \frac{e^{-2\tau\lambda_0} |\langle\lambda_0|\Psi_0\rangle|^2}{\|e^{-\tau\hat{H}}|\Psi_0\rangle\|^2}, \quad (50)$$

where one should recall that $|\Psi_0\rangle$ is the initial state of ITE, see Eq. (32). A lower bound for Eq. (50) can be obtained by upper bounding the ITE normalization

$$\|e^{-\tau\hat{H}}|\Psi_0\rangle\|^2 = \langle\Psi_0|e^{-2\tau\hat{H}}|\Psi_0\rangle = \sum_{j=0}^d |\langle\lambda_j|\Psi_0\rangle|^2 e^{-2\tau\lambda_j} \quad (51)$$

$$= |\langle\lambda_0|\Psi_0\rangle|^2 e^{-2\tau\lambda_0} + \sum_{j=1}^d |\langle\lambda_j|\Psi_0\rangle|^2 e^{-2\tau\lambda_j} \quad (52)$$

$$\leq e^{-2\tau\lambda_0} \left[|\langle\lambda_0|\Psi_0\rangle|^2 + \sum_{m=1}^{\infty} e^{-2\tau m\Delta} \sum_{j:\lambda_j \in \mathcal{M}_m} |\langle\lambda_j|\Psi_0\rangle|^2 \right] \quad (53)$$

$$\leq e^{-2\tau\lambda_0} \left[|\langle\lambda_0|\Psi_0\rangle|^2 + \sum_{m=1}^{\infty} \rho_m(\hat{H}) e^{-2\tau m\Delta} \right] \quad (54)$$

$$\leq e^{-2\tau\lambda_0} (|\langle\lambda_0|\Psi_0\rangle|^2 + \exp(e^{-2\tau\Delta} c_H L) - 1). \quad (55)$$

In Eq. (54) we use a very loose upper bound $|\langle\lambda_j|\Psi_0\rangle| \leq 1$ to insert the density of states $\rho_m(\hat{H})$, and in the last line we invoked Hastings' condition. Finally, we proceed to upper bound $F(|\Psi_0\rangle, |\lambda_0\rangle)$ in Eq. (50):

$$F(|\Psi(\tau)\rangle, |\lambda_0\rangle) \geq \frac{|\langle\lambda_0|\Psi_0\rangle|^2}{|\langle\lambda_0|\Psi_0\rangle|^2 + \exp(e^{-2\tau\Delta} c_H L) - 1} \geq \frac{1}{1 + \delta_H} \geq 1 - \delta_H, \quad (56)$$

where we have set $\delta_H = \frac{\exp(e^{-2\tau\Delta} c_H L) - 1}{|\langle\lambda_0|\Psi_0\rangle|^2}$. Inverting this relation we find that it suffices for imaginary-time evolution to have the duration given by

$$\tau_H = \frac{1}{2\Delta} \log \left(\frac{c_H L}{\log(1 + \delta_H |\langle\lambda_0|\Psi_0\rangle|^2)} \right). \quad (57)$$

In Eq. (56) we defined $\delta_H > 0$ as the desired ground-state infidelity for ITE initialized with a non-zero ground-state overlap $F(|\Psi_0\rangle, |\lambda_0\rangle) = |\langle\lambda_0|\Psi_0\rangle|^2 \neq 0$. If \hat{H} has a unique gapped ground-state and it satisfies Hastings' density of states condition in Eq. (45), then the scaling

$$\tau_H = \log(O(L\delta_H^{-1} |\langle\lambda_0|\Psi_0\rangle|^{-2})) \quad (58)$$

in Eq. (57) suffices for ITE to achieve the desired high fidelity.

III. Double-bracket iteration (DBI) approach to QITE

In the previous section, we established that QITE is a DBF. Importantly, we were able to show two key performance indicators of QITE: the cooling rate as a function of energy variance, and the fact that under Hastings' assumption, one may obtain an exponential convergence for the fidelity of the QITE state to target ground-state. Nevertheless, for both numerical and compilation purposes, it will be necessary to demonstrate these properties for *discretizations* of the DBF method. We begin by considering the discretization which we referred to as *double-bracket iteration* (DBI) though previous works used the name Lie bracket recursions [66].

For the computational purposes of this appendix, we introduce the following notation: denote $|\sigma_0\rangle$ as the initial state fed into a discretized DBI computation, and $\{|\sigma_k\rangle\}_k$ as the sequence of states that solve the QITE DBI, which takes on a recursive form:

$$|\sigma_{k+1}\rangle = e^{s_k[\sigma_k, \hat{H}]}|\sigma_k\rangle. \quad (59)$$

In the above, we have denoted the time step size in the $(k+1)$ -th DBI iteration as s_k . Furthermore, to simplify the notation we use the density matrix representation $\sigma_k = |\sigma_k\rangle\langle\sigma_k|$. The quantities of interest, as in Section II B, are given by the average and variance of energy after k -th DBI iteration:

$$\bar{E}_k = \langle\sigma_k|\hat{H}|\sigma_k\rangle, \quad \text{and} \quad \bar{V}_k = \langle\sigma_k|\hat{H}^2|\sigma_k\rangle - \langle\sigma_k|\hat{H}|\sigma_k\rangle^2. \quad (60)$$

A. Useful lemmas for proving fluctuation-refrigeration relation and fidelity convergence of QITE DBI

1. We will use the following lemma in Sec. III B.

Lemma 6. *Let $\hat{W} = -\hat{W}^\dagger$ and $\hat{H} = \hat{H}^\dagger$. Then*

$$\partial_s^n \left(e^{-s\hat{W}} \hat{H} e^{s\hat{W}} \right) = e^{s\hat{W}} [(\hat{W})^n, \hat{H}] e^{-s\hat{W}}, \quad (61)$$

where $n \in \mathbb{N}$ indicates the order of the derivative and we define the notation for nested commutators

$$[(X)^n, Y] = \left[X, [(X)^{n-1}, Y] \right] \quad \text{with} \quad [(X)^0, Y] = Y, \quad (62)$$

Proof. We prove it by mathematical induction. For the base case $n = 1$, we have

$$\partial_s \left(e^{s\hat{W}} \hat{H} e^{-s\hat{W}} \right) = e^{s\hat{W}} \hat{W} \hat{H} e^{-s\hat{W}} - e^{s\hat{W}} \hat{H} \hat{W} e^{-s\hat{W}} = e^{s\hat{W}} [\hat{W}, \hat{H}] e^{-s\hat{W}} \quad (63)$$

Next, we assume that for some integer $n \geq 1$:

$$\partial_s^n \left(e^{s\hat{W}} \hat{H} e^{-s\hat{W}} \right) = e^{s\hat{W}} [(\hat{W})^n, \hat{H}] e^{-s\hat{W}} \quad (64)$$

The $(n+1)$ -th derivative is then given by

$$\partial_s^{n+1} \left(e^{s\hat{W}} \hat{H} e^{-s\hat{W}} \right) = \partial_s \left(e^{s\hat{W}} [(\hat{W})^n, \hat{H}] e^{-s\hat{W}} \right) \quad (65)$$

$$= e^{s\hat{W}} \hat{W} [(\hat{W})^n, \hat{H}] e^{-s\hat{W}} - e^{s\hat{W}} [(\hat{W})^n, \hat{H}] \hat{W} e^{-s\hat{W}} \quad (66)$$

$$= e^{s\hat{W}} [\hat{W}, [(\hat{W})^n, \hat{H}]] e^{-s\hat{W}}. \quad (67)$$

Using the definition of the nested commutator, we have $[\hat{W}, [(\hat{W})^n, \hat{H}]] = [(\hat{W})^{n+1}, \hat{H}]$, and thus we obtain

$$\partial_s^{n+1} \left(e^{s\hat{W}} \hat{H} e^{-s\hat{W}} \right) = e^{s\hat{W}} [(\hat{W})^{n+1}, \hat{H}] e^{-s\hat{W}}. \quad (68)$$

By induction, the formula holds for all $n \geq 1$. \square

2. Let us consider the state $|\psi\rangle = \hat{H}|\phi\rangle/\|\hat{H}|\phi\rangle\|$. We will use it as follows.

Lemma 7 (Second moment bound). *Let $\hat{A} = \hat{A}^\dagger$, then we have $\langle\phi|\hat{H}\hat{A}\hat{H}|\phi\rangle \leq \langle\phi|\hat{H}^2|\phi\rangle\|\hat{A}\|$.*

Proof. By definition

$$\langle\phi|\hat{H}\hat{A}\hat{H}|\phi\rangle = \langle\phi|\hat{H}^2|\phi\rangle\langle\psi|\hat{A}|\psi\rangle \quad (69)$$

and we use the variational definition of the operator norm. \square

3. Usually, operator norms should be used to bound the proximity of unitaries. However, while in general $\|\hat{H}, \Omega\| \leq 2\|\hat{H}\| \|\Omega\|$ is the standard bound, we can get a much stronger bound as follows.

Lemma 8 (Bracket perturbation). *Let $\hat{H} = \hat{H}^\dagger$ and $\Omega = |\Omega\rangle\langle\Omega|$ then $\|\mathbb{1} - e^{[\hat{H}, \Omega]}\| \leq 2\sqrt{V(\Omega)}$.*

Proof. Following Bhatia [138] or using Eq. (115) of Ref. [32] one can prove

$$\|\mathbb{1} - e^{[\hat{H}, \Omega]}\| \leq \|[\hat{H}, \Omega]\|, \quad (70)$$

which holds for any unitarily invariant norm, in particular the operator norm. By using $\|[\hat{H}, \Omega]\| \leq \|[\hat{H}, \Omega]\|_{\text{HS}}$ and Lemma 9 we obtain the result. \square

Note, that normally upper bounding the operator norm by the Hilbert-Schmidt norm gives exponentially loose bounds. This is not the case here.

4. For QITE, we are often interested in the commutator of the state and the system Hamiltonian. In the case of pure states, we may show that its Hilbert Schmidt norm is related to thermodynamic properties of the state, in particular energy variance.

Lemma 9 (Bracket-variance duality). *For any Hamiltonian $\hat{H} = \hat{H}^\dagger$ and pure state $\Omega = |\Omega\rangle\langle\Omega|$,*

$$\|[\hat{H}, \Omega]\|_{\text{HS}}^2 = 2V(\Omega) = 2\langle\Omega|\hat{H}^2|\Omega\rangle - 2\Omega|\hat{H}|\Omega\rangle^2. \quad (71)$$

Proof. Using the definition of Hilbert-Schmidt norm, we have

$$\|[\hat{H}, \Omega]\|_{\text{HS}}^2 = -\text{Tr}\left((\hat{H}\Omega - \Omega\hat{H})(\hat{H}\Omega - \Omega\hat{H})\right) = -\text{Tr}(\hat{H}\Omega\hat{H}\Omega - \Omega\hat{H}^2\Omega - \hat{H}\Omega\hat{H} + \Omega\hat{H}\Omega\hat{H}). \quad (72)$$

We evaluate the trace in a basis that includes $|\Omega\rangle$ and obtain the result by collecting repeated terms. \square

5. The error term in the linear approximation of the QITE DBI is bounded above by the product of the step size and the energy fluctuations raised to the second power.

Lemma 10. *Let \hat{H} be a Hamiltonian and a density matrix Ω corresponding to a pure state. For any real parameter $r \in \mathbb{R}$ the error associated with the linear approximation of the QITE DBR*

$$\mathcal{R}_r := e^{-r[\hat{H}, \Omega]} - \mathbb{1} + r[\hat{H}, \Omega] \quad (73)$$

satisfies $\|\mathcal{R}_r\|_{\text{HS}} \leq r^2 \bar{V}_k$.

Proof. Using Taylor's theorem we have

$$\mathcal{R}_r = \mathcal{R}_0 + \int_0^r dx \partial_x \mathcal{R}_x = \int_0^r dx [\hat{H}, \Omega] \left(\mathbb{1} - e^{-x[\hat{H}, \Omega]} \right), \quad (74)$$

where we use the fact that $\mathcal{R}_0 = 0$. Taking the Hilbert-Schmidt norm for the last expression becomes

$$\|\mathcal{R}_r\|_{\text{HS}} = \left\| \int_0^r dx [\hat{H}, \Omega] (\mathbb{1} - e^{-x[\hat{H}, \Omega]}) \right\|_{\text{HS}} \leq \|[\hat{H}, \Omega]\|_{\text{HS}} \times \left\| \int_0^r dx (\mathbb{1} - e^{-x[\hat{H}, \Omega]}) \right\|_{\text{HS}}. \quad (75)$$

Set $[H, \Omega] \rightarrow x[H, \Omega]$ in Lemma. 8, we have

$$\left\| \mathbb{1} - e^{-x[H, \Omega]} \right\|_{\text{HS}} \leq x \| [H, \Omega] \|_{\text{HS}}. \quad (76)$$

Thus, it simplifies to

$$\|\mathcal{R}_r\|_{\text{HS}} \leq \| [H, \Omega] \|_{\text{HS}}^2 \times \left\| \int_0^r dx x \right\|_{\text{HS}} = \frac{r^2}{2} \| [H, \Omega] \|_{\text{HS}}^2. \quad (77)$$

Using Lemma. 9, we then obtain $\|\mathcal{R}_r\|_{\text{HS}} \leq r^2 \bar{V}_k$. \square

B. Proof of fluctuation-refrigeration relation for QITE DBI and its cooling rate

In this section, we derive the cooling rate of QITE state by using DBI implementation.

Proposition 11 (QITE-DBI Fluctuation-refrigeration relation). *Let $\{|\sigma_k\rangle\}_k$ be a sequence of states that solve the QITE-DBI relation in Eq. (8). The first-order cooling rate of QITE DBI equals that of QITE*

$$\bar{E}_{k+1} - \bar{E}_k \leq -2s_k \bar{V}_k + \mathcal{O}(s_k^2). \quad (78)$$

If each time step is chosen such that $s_k \leq \frac{\bar{V}_k}{4\|\hat{H}\|\langle\sigma_k|\hat{H}^2|\sigma_k\rangle}$, then the DBI cooling rate is lower bounded as

$$\bar{E}_{k+1} - \bar{E}_k \leq -s_k \bar{V}_k, \quad (79)$$

where the average energies \bar{E}_k and variances \bar{V}_k are defined in Eq. (60).

Proof. Let us begin by defining the average energy of the k -th DBI state as a function of the time step s ,

$$\bar{E}_k(s) = \langle\sigma_k|e^{-s[\sigma_k, \hat{H}]} \hat{H} e^{s[\sigma_k, \hat{H}]}|\sigma_k\rangle. \quad (80)$$

Note that the derivative of $\bar{E}_k(s)$ when evaluated at $s = 0$ gives $\partial_s \bar{E}_k(0) = -2\bar{V}_k$, exactly as in Proposition. 5. The difference in factor 2 here is that we need to provide a lower bound to the cooling rate for a finite double-bracket rotation duration $s \neq 0$.

By using a Taylor expansion on Eq. (80), we find

$$\bar{E}_k(s_k) = \bar{E}_k + s_k \partial_s \bar{E}_k(s)|_{s=0} + \frac{1}{2} s_k^2 \partial_s^2 \bar{E}_k(s)|_{s=\xi_k}, \quad (81)$$

where $\xi_k \in [0, s_k]$ is the point of the Lagrange remainder (point 6, Sec. I). Next, recall that $\bar{E}_k(s_k)$ is simply equal to \bar{E}_{k+1} by definition, hence

$$\bar{E}_{k+1} - \bar{E}_k = s_k \partial_s \bar{E}_k(s)|_{s=0} + \frac{1}{2} s_k^2 \partial_s^2 \bar{E}_k(s)|_{s=\xi_k}. \quad (82)$$

To simplify the notation, it is convenient to use the following shorthands

$$\hat{W}_k = [\sigma_k, \hat{H}], \quad \hat{H}_k(s) = e^{-s\hat{W}_k} \hat{H} e^{s\hat{W}_k}. \quad (83)$$

Note that $e^{-s\hat{W}_k}$ is unitary, and hence $\|\hat{H}_k(s)\| = \|\hat{H}\|$. The 1st order derivative of average energy is then given by $\partial_s \bar{E}_k(s) = \langle\sigma_k|[\hat{H}_k(s), \hat{W}_k]|\sigma_k\rangle$. Expanding this yields for $s = 0$

$$\partial_s \bar{E}_k(s)|_{s=0} = \langle\sigma_k|(\hat{H}\sigma_k\hat{H} - \hat{H}^2\sigma_k - \sigma_k\hat{H}^2 + \hat{H}\sigma_k\hat{H})|\sigma_k\rangle \quad (84)$$

$$= -2\langle\sigma_k|\hat{H}^2|\sigma_k\rangle + 2\bar{E}_k^2 = -2\bar{V}_k \leq 0. \quad (85)$$

For the 2nd order derivative, we use a double-nested commutator Eq. (61) and by explicit computation

$$\partial_s^2 \bar{E}_k(s) = \langle\sigma_k|[[\hat{H}_k(s), \hat{W}_k], \hat{W}_k]|\sigma_k\rangle \quad (86)$$

$$= \langle\sigma_k|\hat{H}_k(s)\hat{W}_k^2|\sigma_k\rangle + \langle\sigma_k|\hat{W}_k^2\hat{H}_k(s)|\sigma_k\rangle - 2\langle\sigma_k|\hat{W}_k\hat{H}_k(s)\hat{W}_k|\sigma_k\rangle, \quad (87)$$

where we commuted \hat{W}_k 's with its exponentials. Next, we will use

$$\hat{W}_k^2|\sigma_k\rangle = (\sigma_k\hat{H}\sigma_k\hat{H} - \sigma_k\hat{H}^2)|\sigma_k\rangle \quad (88)$$

to expand the DBI brackets. This gives us

$$\begin{aligned} \partial_s^2 \bar{E}_k(s) &= \langle\sigma_k|\hat{H}_k(s)\sigma_k\hat{H}\sigma_k\hat{H}|\sigma_k\rangle - \langle\sigma_k|\hat{H}_k(s)\sigma_k\hat{H}^2|\sigma_k\rangle + \langle\sigma_k|\hat{H}\sigma_k\hat{H}\sigma_k\hat{H}_k(s)|\sigma_k\rangle - \langle\sigma_k|\hat{H}^2\sigma_k\hat{H}_k(s)|\sigma_k\rangle \\ &\quad - 2\langle\sigma_k|\hat{H}\hat{H}_k(s)\sigma_k\hat{H}|\sigma_k\rangle + 2\langle\sigma_k|\hat{H}\hat{H}_k(s)\hat{H}|\sigma_k\rangle + 2\langle\sigma_k|\hat{H}\sigma_k\hat{H}_k(s)\sigma_k\hat{H}|\sigma_k\rangle - 2\langle\sigma_k|\hat{H}\sigma_k\hat{H}_k(s)\hat{H}|\sigma_k\rangle \end{aligned} \quad (89)$$

$$= -2\bar{V}_k \bar{E}_k(s) + 2\langle\sigma_k|\hat{H}\hat{H}_k(s)\hat{H}|\sigma_k\rangle + 2\bar{E}_k^2 \bar{E}_k(s) - 4\bar{E}_k \text{Re}(\langle\sigma_k|\hat{H}\hat{H}_k(s)|\sigma_k\rangle). \quad (90)$$

The first term is negative so reduces the energy of the state (to 2nd order). The second term can be bound using Lemma 7 as

$$|\langle\sigma_k|\hat{H}\hat{H}_k(s)\hat{H}|\sigma_k\rangle| \leq \langle\sigma_k|\hat{H}^2|\sigma_k\rangle \|\hat{H}_k(s)\| \leq \langle\sigma_k|\hat{H}^2|\sigma_k\rangle \|\hat{H}\|. \quad (91)$$

To bound the last term in Eq. (90), we have

$$|\operatorname{Re}(\langle \sigma_k | \hat{H} \hat{H}_k(s) | \sigma_k \rangle)| \leq |\langle \hat{H} | \sigma_k \rangle, \hat{H}_k(s) | \sigma_k \rangle| \leq \sqrt{\langle \sigma_k | \hat{H}^2 | \sigma_k \rangle} \sqrt{\langle \sigma_k | \hat{H}_k(s)^2 | \sigma_k \rangle} \quad (92)$$

$$\leq \sqrt{\langle \sigma_k | \hat{H}^2 | \sigma_k \rangle} \|\hat{H}\|, \quad (93)$$

where we used Cauchy-Schwarz in the second inequality. Therefore, we have

$$\partial_s^2 \bar{E}_k(s) \leq -2\bar{V}_k \bar{E}_k(s) + 2\bar{E}_k^2 \|\hat{H}\| + 4\bar{E}_k \sqrt{\langle \sigma_k | \hat{H}^2 | \sigma_k \rangle} \|\hat{H}\| + 2\langle \sigma_k | \hat{H}^2 | \sigma_k \rangle \|\hat{H}\| \leq 8\langle \sigma_k | \hat{H}^2 | \sigma_k \rangle \|\hat{H}\|. \quad (94)$$

As a remark, from the end of Eq. (94) we can obtain a weaker bound by using the sub-multiplicativity of the operator norm, i.e. we have $\partial_s^2 \bar{E}_k(s) \leq 8\|\hat{H}\|^3$. Finally, we have

$$\bar{E}_{k+1} - \bar{E}_k \leq -2s_k \bar{V}_k + 4s_k^2 \langle \sigma_k | \hat{H}^2 | \sigma_k \rangle \|\hat{H}\|, \quad (95)$$

so as we place the constraint that $-s_k \bar{V}_k + 4s_k^2 \langle \sigma_k | \hat{H}^2 | \sigma_k \rangle \|\hat{H}\| \leq 0$, this leads to $\bar{E}_{k+1} - \bar{E}_k \leq -s_k \bar{V}_k$. Evaluating the constraint as an upper bound on s_k , we obtain $s_k \leq \frac{\bar{V}_k}{4\|\hat{H}\| \langle \sigma_k | \hat{H}^2 | \sigma_k \rangle}$. \square

Remark. Scrutinizing Eq. (90) around $s = 0$ allows us to further see the significance of higher moments of energy distribution, for the purposes of QITE. In particular, using Eq. (90), we have

$$\partial_s^2 \bar{E}_k(s)|_{s=0} = -2\bar{V}_k \bar{E}_k + 2\langle \sigma_k | \hat{H}^3 | \sigma_k \rangle + 2\bar{E}_k^2 \bar{E}_k - 4\bar{E}_k \langle \sigma_k | \hat{H}^2 | \sigma_k \rangle \quad (96)$$

$$= 2\left(\langle \sigma_k | \hat{H}^3 | \sigma_k \rangle - \bar{V}_k \bar{E}_k + \bar{E}_k^3 - 2\bar{E}_k(\bar{V}_k + \bar{E}_k^2)\right) \quad (97)$$

$$= 2\left(\langle \sigma_k | \hat{H}^3 | \sigma_k \rangle - 3\bar{E}_k \bar{V}_k - \bar{E}_k^3\right) = 2\langle \sigma_k | (\hat{H} - \bar{E}_k)^3 | \sigma_k \rangle, \quad (98)$$

because one can verify that

$$\langle \sigma_k | (\hat{H} - \bar{E}_k)^3 | \sigma_k \rangle = \langle \sigma_k | \hat{H}^3 | \sigma_k \rangle - 3\langle \sigma_k | \hat{H}^2 \bar{E}_k | \sigma_k \rangle + 3\langle \sigma_k | \hat{H} \bar{E}_k^2 | \sigma_k \rangle - \langle \sigma_k | \bar{E}_k^3 | \sigma_k \rangle \quad (99)$$

$$= \langle \sigma_k | \hat{H}^3 | \sigma_k \rangle - 3\bar{E}_k \bar{V}_k - \bar{E}_k^3. \quad (100)$$

Combining Eq. (85) and Eq. (98), the Taylor expansion of the expected energy is given by

$$\bar{E}_k(s) = \bar{E}_k - 2s\langle \sigma_k | (\hat{H} - \bar{E}_k)^2 | \sigma_k \rangle + s^2\langle \sigma_k | (\hat{H} - \bar{E}_k)^3 | \sigma_k \rangle + \mathcal{O}(s^3). \quad (101)$$

This means that whenever skewness is negative, then one can analytically justify longer double-bracket rotation durations – the second order term would then enhance cooling process for the state.

C. Exponential fidelity convergence of QITE DBI

Lemma 12 (Lower bound to energy over variance). *Let $|\Omega\rangle$ be any pure state. Denote Hamiltonian as $\hat{H} = \sum_{j=0}^{d-1} \lambda_j |\lambda_j\rangle\langle\lambda_j|$ where we assume that the eigenvalues of \hat{H} are ordered increasingly and that $\lambda_0 = 0$. Suppose that the ground-state fidelity is given by $F = 1 - \epsilon$, then we have*

$$\frac{E}{V} \geq \frac{1}{\|\hat{H}\|}, \quad (102)$$

where $E = \langle \Omega | \hat{H}^2 | \Omega \rangle$ is the expected energy and $V = \langle \Omega | \hat{H}^2 | \Omega \rangle - E^2$ is the energy variance.

Proof. Let us define the probability to occupy the i -th eigenstate $p_i := |\langle \lambda_i | \Omega \rangle|^2$. Since $\lambda_0 = 0$ by assumption, we obtain

$$E - \frac{V}{\|\hat{H}\|} = \sum_{i=1}^{d-1} \lambda_i p_i - \frac{1}{\|\hat{H}\|} \sum_{i=1}^{d-1} \lambda_i^2 p_i + \frac{1}{\|\hat{H}\|} \left(\sum_{i=1}^{d-1} \lambda_i p_i \right)^2 \quad (103)$$

$$\geq \sum_{i=1}^{d-1} \left(1 - \frac{\lambda_i}{\|\hat{H}\|} \right) \lambda_i p_i \geq 0. \quad (104)$$

\square

Remark. This bound is (asymptotically) tight for $\epsilon \rightarrow 0$. Indeed, if $p_{d-1} = \epsilon$ and $p_i = 0$ for $i < d-1$, we obtain

$$\frac{E}{V} = \frac{\lambda_{d-1}\epsilon}{\lambda_{d-1}^2\epsilon - \lambda_{d-1}^2\epsilon^2} = \frac{1}{\|\hat{H}\|(1-\epsilon)} \quad (105)$$

This lemma can be used to prove the following result.

Theorem 13 (Exponential fidelity convergence for QITE DBI). *Let $\hat{H} = \sum_{j=0}^{d-1} \lambda_j |\lambda_j\rangle\langle\lambda_j|$ be a Hamiltonian where $d = \dim(\hat{H})$, $\{|\lambda_i\rangle\}$ is the set of increasingly ordered eigenstates with $\lambda_0 = 0$ and we denote the ground state by $|\lambda_0\rangle$. Let $|\sigma_0\rangle$ be an initial state with non-zero overlap to the ground-state, where the fidelity is given by $F_0 = |\langle\lambda_0|\sigma_0\rangle|^2$. Consider QITE DBI with*

$$|\sigma_{k+1}\rangle = e^{s_0[|\sigma_k\rangle\langle\sigma_k|, \hat{H}]} |\sigma_k\rangle, \quad (106)$$

where $s_0 = \sqrt{F_0}/(4\lambda_{d-1})$ is the same in all steps. The fidelity for the k -th DBI step defined by $F_k = |\langle\lambda_0|\sigma_k\rangle|^2$ satisfies

$$F_k \geq 1 - q^k, \text{ where } q = 1 - \left(\frac{1}{4} \frac{\lambda_1}{\lambda_{d-1}} F_0^{\frac{3}{2}} \right) = 1 - \left(\frac{1}{4} \frac{\lambda_1}{\|\hat{H}\|} F_0^{\frac{3}{2}} \right). \quad (107)$$

The convergence rate is set by a quantity related to the condition number of the Hamiltonian which also appears in classical algorithms. For a non-singular matrix A the condition number is defined as $\kappa(A) = \|A^{-1}\| \|A\|$. In our problem, we have affine invariance $\hat{H} \mapsto \hat{H} + \alpha \mathbb{I}$ which does not change the ground-state state vector $|\lambda_0\rangle$ or the dynamics of the Hamiltonian. Observe that DBIs are invariant under affine shifts of the Hamiltonian, in particular we have $[\hat{H} - \lambda_0 \mathbb{I}, \sigma_k] = [\hat{H}, \sigma_k]$ which means that $\hat{H}' = \hat{H} - \lambda_0 \mathbb{I}$ with vanishing ground-state energy $\hat{H}'|\lambda_0\rangle = 0$ has the same DBI unitaries. Thus, without loss of generality, we assume the ground-state to be zero, i.e. $\lambda_0 = 0$. In that case, a more meaningful notion of the condition number is

$$\kappa_0(\hat{H}) = \lambda_{d-1}/\lambda_1. \quad (108)$$

In classical numerical analysis we have $\kappa(A) \geq 1$ and whenever $\kappa(A)$ is large then A is considered badly conditioned. Using this notation allows us to write

$$q = 1 - \left(\frac{1}{4} \frac{F_0^{\frac{3}{2}}}{\kappa_0(\hat{H})} \right). \quad (109)$$

If $\kappa_0(\hat{H})$ is large, which for local Hamiltonians corresponds to a small spectral gap, then the QITE DBI converges more slowly.

Proof. Next, the ground-state fidelity after each round of QITE DBI iteration is given by

$$F_{k+1} = |\langle\lambda_0|\sigma_{k+1}\rangle|^2 = \left| \langle\lambda_0|\sigma_k\rangle - s_0 \langle\lambda_0|[\hat{H}, \sigma_k]|\sigma_k\rangle + \langle\lambda_0|R|\sigma_k\rangle \right|^2 \quad (110)$$

$$= \left| \langle\lambda_0|\sigma_k\rangle (1 + s_0 \langle\sigma_k|\hat{H}|\sigma_k\rangle) - s_0 \langle\lambda_0|\hat{H}|\sigma_k\rangle + \langle\lambda_0|R|\sigma_k\rangle \right|^2 \quad (111)$$

$$= \left| \langle\lambda_0|\sigma_k\rangle (1 + s_0 \overline{E}_k) + \langle\lambda_0|R|\sigma_k\rangle \right|^2, \quad (112)$$

where R denotes the error term of the linear approximation to the QITE DBI. Since we set $\lambda_0 = 0$, the term $s_0 \langle\lambda_0|\hat{H}|\sigma_k\rangle$ vanishes. Furthermore, note that $|\langle\lambda_0|\sigma_k\rangle|^2 = F_k$. Hence we have

$$F_{k+1} = F_k (1 + s_0 \overline{E}_k)^2 + 2(1 + s_0 \overline{E}_k) \text{Re} \left(\langle\lambda_0|\sigma_k\rangle \langle\sigma_k|R^\dagger|\lambda_0\rangle \right) + |\langle\lambda_0|R|\sigma_k\rangle|^2. \quad (113)$$

Next, note that $0 \leq |\langle\lambda_0|R|\sigma_k\rangle|^2 \leq \|R\|_{\text{HS}}^2 = \|R^\dagger\|_{\text{HS}}^2 \leq s_0^2 V_k$ by Lemma 10. Thus, Eq. (113) becomes

$$F_{k+1} \geq F_k (1 + s_0 \overline{E}_k)^2 - 2s_0^2 \overline{V}_k \left(1 + s_0 \overline{E}_k \right) \sqrt{F_k}, \quad (114)$$

where we dropped the third term in Eq. (113), and use the bound $\langle\sigma_k|R^\dagger|\lambda_0\rangle \geq -\|R^\dagger\|_{\text{HS}} \geq -s_0^2 \overline{V}_k$.

Using the definition of the infidelity $F_k = 1 - \epsilon_k$, we can rewrite it as

$$1 - \epsilon_{k+1} \geq (1 - \epsilon_k)(1 + s_0 \bar{E}_k)^2 - 2s_0^2 \bar{V}_k \left(1 + s_0 \bar{E}_k\right) \sqrt{1 - \epsilon_k} \quad (115)$$

$$\epsilon_{k+1} \leq 1 - (1 - \epsilon_k)(1 + s_0 \bar{E}_k)^2 + 2s_0^2 \bar{V}_k \left(1 + s_0 \bar{E}_k\right) \sqrt{1 - \epsilon_k} \quad (116)$$

$$\leq \epsilon_k - 2s_0 \bar{E}_k (1 - \epsilon_k) - s_0^2 \bar{E}_k^2 (1 - \epsilon_k) + 2s_0^2 \bar{V}_k \left(1 + s_0 \bar{E}_k\right) \sqrt{1 - \epsilon_k} \quad (117)$$

$$\leq \epsilon_k - 2s_0 \bar{E}_k (1 - \epsilon_k) + 2s_0^2 \bar{V}_k \left(1 + s_0 \bar{E}_k\right) \sqrt{1 - \epsilon_k} . \quad (118)$$

Next, note that according to the assumed form s_0 in the theorem statement, and the fact that $\bar{E}_k \leq \|H\| = \lambda_{d-1}$, we have that $s_0 \bar{E}_k \leq \frac{1}{4} \frac{\sqrt{F_0}}{\lambda_{d-1}} \lambda_{d-1} \leq 1$, so we can simplify the above bound by relaxing it further:

$$\epsilon_{k+1} \leq \epsilon_k - 2s_0 \bar{E}_k (1 - \epsilon_k) + 4s_0^2 \bar{V}_k \sqrt{1 - \epsilon_k} . \quad (119)$$

Our goal is to suppress the second-order term by utilizing half of the first-order infidelity reduction. To do so, the condition $4s_0^2 \bar{V}_k \sqrt{1 - \epsilon_k} \leq s_0 \bar{E}_k (1 - \epsilon_k)$ must be satisfied, which is equivalent to $s_0 \leq \bar{E}_k \sqrt{1 - \epsilon_k} / (4\bar{V}_k)$. Next, from Lemma. 12, we have $\bar{E}_k / \bar{V}_k \geq 1 / \lambda_{d-1}$. Using this bound, we can verify that indeed,

$$s_0 = \frac{1}{4} \frac{\sqrt{F_0}}{\lambda_{d-1}} \leq \frac{\bar{E}_k}{4\bar{V}_k} \sqrt{1 - \epsilon_k} . \quad (120)$$

Since the condition $s_0 \leq \bar{E}_k \sqrt{1 - \epsilon_k} / (4\bar{V}_k)$ holds, Eq. (119) can be directly upper-bounded by

$$\epsilon_{k+1} \leq \epsilon_k - s_0 \bar{E}_k F_0 . \quad (121)$$

In Eq. (120) we assume that $\epsilon_k \leq \epsilon_0$. Clearly, this is satisfied for $k = 0$, and can be concluded for $k > 0$ by induction on k using Eq. (121). Finally, using the definition of s_0 , we have that the error reduces to

$$\epsilon_{k+1} \leq \epsilon_k - \frac{1}{4} \frac{\lambda_1}{\lambda_{d-1}} F_0^{\frac{3}{2}} \epsilon_k = \left(1 - \left(\frac{1}{4} \frac{\lambda_1}{\lambda_{d-1}} F_0^{\frac{3}{2}}\right)\right) \epsilon_k , \quad (122)$$

where we use the relation $\bar{E}_k \geq \lambda_1 \epsilon_k$ from Lemma. 3. \square

IV. Double-Bracket Quantum Imaginary-Time Evolution (DB-QITE)

In Sec. II and Sec. III, we consider the QITE realization via the continuous DBF and discrete DBI method. Here, we aim to employ the discrete group commutator iteration (GCI) to approximate DBI. As demonstrated in Lemma. (9) from [32], we can approximate DBI steps by group-commutators with an error term of magnitude $\mathcal{O}(s_k^{3/2})$, i.e. we have

$$\left\| e^{i\sqrt{s_k}\hat{H}} e^{i\sqrt{s_k}\omega_k} e^{-i\sqrt{s_k}\hat{H}} e^{-i\sqrt{s_k}\omega_k} - e^{s_k[\omega_k, \hat{H}]} \right\| \leq s_k^{3/2} \left(\|\hat{H}, [\hat{H}, \omega_k]\| + \|[\omega_k, [\omega_k, \hat{H}]]\| \right) , \quad (123)$$

where $\|\cdot\|$ represents the operator norm, and k denotes the number of iteration in both DBI and GCI. Next, observe that $e^{-i\sqrt{s_k}\omega_k} |\omega_k\rangle = e^{-i\sqrt{s_k}\omega_k} |\omega_k\rangle$ which motivates the definition of the *reduced group-commutator iteration (DB-QITE)*:

$$|\omega_{k+1}\rangle = e^{i\sqrt{s_k}\hat{H}} e^{i\sqrt{s_k}\omega_k} e^{-i\sqrt{s_k}\hat{H}} |\omega_k\rangle . \quad (124)$$

This is essentially Eq. (12) in the main text, but in general one can optimize the individual step sizes s_k in each round. Lastly, we denote the expected energy and variance after the k -th round of DB-QITE as

$$E_k = \langle \omega_k | \hat{H} | \omega_k \rangle \quad \text{and} \quad V_k = \langle \omega_k | \hat{H}^2 | \omega_k \rangle - \langle \omega_k | \hat{H} | \omega_k \rangle^2 . \quad (125)$$

Intuitively due to Eq. (123), one expects a qualitatively similar behavior between DB-QITE and DBF/DBI. We derive quantitative bounds in the next sections, to compare their explicit differences.

Before proving the main results in this section, i.e. analytical guarantees for energy loss and fidelity improvement in DB-QITE implementation, let's first present two key lemmas that will be handy in the proof.

Lemma 14. Suppose that the DB-QITE state $|\omega_k\rangle$ is a pure state, then we have the following equivalent representation for the next DB-QITE state $|\omega_{k+1}\rangle$:

$$|\omega_{k+1}\rangle = e^{i\sqrt{s_k}\hat{H}} e^{i\sqrt{s_k}\omega_k} e^{-i\sqrt{s_k}\hat{H}} |\omega_k\rangle \iff |\omega_{k+1}\rangle = \left(\mathbb{1} - (\mathbb{1} - e^{i\sqrt{s_k}})\phi(-\sqrt{s_k})e^{i\sqrt{s_k}\hat{H}} \right) |\omega_k\rangle, \quad (126)$$

where we define the characteristic function as

$$\phi(t) := \langle \omega_k | e^{it\hat{H}} | \omega_k \rangle. \quad (127)$$

Proof. Since we consider a pure state $\omega_k = |\omega_k\rangle\langle\omega_k|$, we obtain the following identity

$$e^{i\sqrt{s_k}\omega_k} = \mathbb{1} - (1 - e^{i\sqrt{s_k}})\omega_k. \quad (128)$$

Therefore, the DB-QITE recursion can be simplified to

$$|\omega_{k+1}\rangle = e^{i\sqrt{s_k}\hat{H}} \left(\mathbb{1} - (1 - e^{i\sqrt{s_k}})\omega_k \right) e^{-i\sqrt{s_k}\hat{H}} |\omega_k\rangle \quad (129)$$

$$= |\omega_k\rangle - (1 - e^{i\sqrt{s_k}})e^{i\sqrt{s_k}\hat{H}} |\omega_k\rangle\langle\omega_k| e^{-i\sqrt{s_k}\hat{H}} |\omega_k\rangle \quad (130)$$

$$= \left(\mathbb{1} - (1 - e^{i\sqrt{s_k}})\phi(-\sqrt{s_k})e^{i\sqrt{s_k}\hat{H}} \right) |\omega_k\rangle, \quad (131)$$

where we use the density matrix representation in the second line and the definition of the characteristic function in the last line. \square

Lemma 15. Denote the characteristic function as $\phi(t) := \langle \omega_k | e^{it\hat{H}} | \omega_k \rangle$. Then the n -th derivative of $\phi(t)$ can be upper-bounded by

$$|\phi^{(n)}(\xi)| \leq \|\hat{H}^n\|, \quad (132)$$

where $\xi \in [0, t]$. Moreover, suppose one knows the ground-state infidelity $\epsilon_k = 1 - F_k$ at k -th QITE DBQA iteration, then we can obtain a tighter bound for $|\phi^{(n)}(\xi)|$, i.e.

$$|\phi^{(n)}(\xi)| \leq \epsilon_k \|\hat{H}^n\|. \quad (133)$$

Proof. Directly evaluating the n -th order derivative of $\phi(t)$ gives

$$\phi^{(n)}(\xi) = i^n \langle \omega_k | e^{i\xi\hat{H}} \hat{H}^n | \omega_k \rangle. \quad (134)$$

As the operator norm is equal to the largest eigenvalue, we obtain the bound

$$|\phi^{(n)}(\xi)| = |\langle \omega_k | e^{i\xi\hat{H}} \hat{H}^n | \omega_k \rangle| \leq \|e^{i\xi\hat{H}} \hat{H}^n\| = \|\hat{H}^n\|, \quad (135)$$

where we use the unitary invariant property of the operator norm in the last equality and neglect the factor i^n as it is of norm 1. Thus, the first part of this lemma has been proven.

Next, to prove the second part, we denote Π_0, Π_\perp as the ground-state projector and its complement (i.e. $\Pi_0 + \Pi_\perp = \mathbb{1}$), then $F_k = \langle \omega_k | \Pi_0 | \omega_k \rangle$ and $\epsilon_k = \langle \omega_k | \Pi_\perp | \omega_k \rangle$. Therefore, we obtain

$$|\phi^{(n)}(\xi)| = |\langle \omega_k | e^{i\xi\hat{H}} \hat{H}^n | \omega_k \rangle| \leq |\langle \omega_k | \Pi_0 e^{i\xi\hat{H}} \hat{H}^n | \omega_k \rangle| + |\langle \omega_k | \Pi_\perp e^{i\xi\hat{H}} \hat{H}^n | \omega_k \rangle| \quad (136)$$

$$= |\langle \omega_k | \Pi_\perp e^{i\xi\hat{H}} \hat{H}^n | \omega_k \rangle| \leq \epsilon_k \|\hat{H}^n\|, \quad (137)$$

where in the last inequality, one may expand the projector and use the fact that $\hat{H}^n e^{i\xi\hat{H}} |\lambda_j\rangle = \lambda_j^n e^{i\xi\lambda_j} |\lambda_j\rangle$ and that $\lambda_j^n \leq \lambda_{d-1}^n$ (recall that λ_{d-1} is the largest energy eigenvalue). \square

A. Fluctuation-refrigeration relation of DB-QITE

Theorem 16. DB-QITE satisfies the fluctuation-refrigeration up to correction terms,

$$E_{k+1} \leq E_k - 2s_k V_k + \mathcal{O}(s_k^2). \quad (138)$$

In particular, if the step sizes are chosen such that $s_k \leq 2V_k \cdot \left[5\epsilon_k \|\hat{H}\|^4 \right]^{-1}$, then $E_{k+1} \leq E_k - s_k V_k$.

Proof. We start from RHS of Eq. (126), i.e.

$$|\omega_{k+1}\rangle = \left(\mathbb{1} - (1 - e^{i\sqrt{s_k}})\phi(-\sqrt{s_k})e^{i\sqrt{s_k}\hat{H}} \right) |\omega_k\rangle, \quad (139)$$

where we employ the same notation for the characteristic function defined in Eq. (127), i.e.

$$\phi(t) := \langle \omega_k | e^{it\hat{H}} | \omega_k \rangle. \quad (140)$$

To simplify calculational notation, we drop the square root and index from step sizes, i.e. $\sqrt{s_k} \rightarrow t$ for the moment. Moreover, we define $c = (1 - e^{it})\phi(-t)$ and hence we have

$$|\omega_{k+1}\rangle = (\mathbb{1} - ce^{it\hat{H}})|\omega_k\rangle. \quad (141)$$

To derive the cooling rate, we calculate

$$E_{k+1} = \langle \omega_{k+1} | \hat{H} | \omega_{k+1} \rangle = \langle \omega_k | \left[\mathbb{1} - c^* e^{-it\hat{H}} \right] \cdot \hat{H} \cdot \left[\mathbb{1} - ce^{it\hat{H}} \right] | \omega_k \rangle \quad (142)$$

$$= E_k + |c|^2 E_k - 2\text{Re} \left(\langle \omega_k | ce^{it\hat{H}} \hat{H} | \omega_k \rangle \right), \quad (143)$$

where we have already made use of the fact that \hat{H} commutes with $e^{-it\hat{H}}$. To achieve Eq. (138), we need to derive upper bounds from Eq. (143), which we do for the individual terms:

1. The second term on the R.H.S. of Eq. (143) can be upper bounded by the fact that

$$|c|^2 = |(1 - e^{it})\phi(-t)|^2 \leq |1 - e^{it}|^2 \cdot |\phi(-t)|^2 \leq t^2, \quad (144)$$

since $(1 - e^{it})(1 - e^{-it}) = 2(1 - \cos(t)) \leq t^2$, and $|\phi(-t)| \leq \|e^{-it\hat{H}}\| \leq 1$.

2. The third term in Eq. (143) can be rewritten as

$$f(t) := -2\text{Re} \left(c \langle \omega_k | e^{it\hat{H}} \hat{H} | \omega_k \rangle \right) = -2\text{Re} \left((1 - e^{it}) \cdot \langle \omega_k | e^{-it\hat{H}} | \omega_k \rangle \cdot \langle \omega_k | e^{it\hat{H}} \hat{H} | \omega_k \rangle \right) \quad (145)$$

$$= -2\text{Im} \left[(1 - e^{it})\phi(-t)\phi^{(1)}(t) \right], \quad (146)$$

since the first derivative of $\phi(t)$ with respect to t is given by $\phi^{(1)}(t) = i\langle \omega_k | e^{it\hat{H}} \hat{H} | \omega_k \rangle$. Our grand goal is to upper bound this term. At this point, let us note that $f(t)$ is an even function with $f(0) = 0$. We may then omit odd derivatives of it, and write the following Taylor expansion,

$$f(t) = \frac{f^{(2)}(0)}{2}t^2 + \frac{f^{(4)}(0)}{24}t^4. \quad (147)$$

To access the higher derivatives of $f(t)$, we start by defining

$$h(t) := \phi(-t)\phi^{(1)}(t), \quad (148)$$

and write derivatives of $f(t)$ as

$$f^{(2)}(t) = -2\text{Im} \left[e^{it}h(t) - 2ie^{it}h^{(1)}(t) + (1 - e^{it})h^{(2)}(t) \right], \quad (149)$$

$$f^{(4)}(t) = -2\text{Im} \left[-e^{it}h(t) + 4ie^{it}h^{(1)}(t) + 6e^{it}h^{(2)}(t) - 4ie^{it}h^{(3)}(t) + (1 - e^{it})h^{(4)}(t) \right]. \quad (150)$$

i) Evaluating $f^{(2)}(0)$ in Eq. (149)

The first term is easy; we have explicitly derived $f^{(2)}(t)$ in Eq. (149), and we need the expression for $h(t)$ as detailed in Eq. (148) and (140). In particular, one can verify that $h(0) = iE_k$ and $h^{(1)}(0) = -V_k$. Therefore, we have

$$f^{(2)}(0) = -2\text{Im} \left[h(0) - 2ih^{(1)}(0) \right] = -2E_k - 4V_k. \quad (151)$$

At this point, it is good to note that by combining Eqns. (144) and Eq. (151) into the equation for cooling, i.e. Eq. (143),

$$E_{k+1} \leq E_k - 2V_k t^2 + \frac{f^{(4)}(\xi)}{24} t^4 = E_k - V_k t^2 - V_k t^2 + \frac{f^{(4)}(\xi)}{24} t^4, \quad (152)$$

which will give us the desired fluctuation-refrigeration relation $E_{k+1} \leq E_k - V_k t^2$ if we can choose t such that

$$-V_k t^2 + \frac{f^{(4)}(\xi)}{24} t^4 \leq 0 \quad \implies \quad t^2 \leq \frac{24V_k}{f^{(4)}(\xi)}. \quad (153)$$

In other words, our next step is to formulate an upper bound $f^{(4)}(\xi) \leq X$, such that by choosing $t^2 \leq \frac{24V_k}{X}$, we complete the proof.

ii) Upper bounding $f^{(4)}(t)$ in Eq. (150)

We proceed to carefully bound each individual term contained in $f^{(4)}(t)$, since

$$f^{(4)}(t) = -2\text{Im} \left[-e^{it}h(t) + 4ie^{it}h^{(1)}(t) + 6e^{it}h^{(2)}(t) - 4ie^{it}h^{(3)}(t) + (1 - e^{it})h^{(4)}(t) \right] \quad (154)$$

$$\leq 2 \left[|h(t)| + 4|h^{(1)}(t)| + 6|h^{(2)}(t)| + 4|h^{(3)}(t)| + |(1 - e^{-it})h^{(4)}(t)| \right], \quad (155)$$

where note that most e^{it} terms are omitted since its norm is bounded by 1. Recall that $h(t)$ is defined in Eq. (148) in terms of derivatives of $\phi(t)$, and so $h^{(n)}(t)$ needs to be explicitly derived as functions containing derivatives of $\phi(t)$ via chain rule. To bound the term $h^{(n)}(t)$, we first recall the bound of $|\phi^{(n)}(\xi)|$ from Eq. (132) in Lemma. 15, i.e.

$$|\phi^{(n)}(\xi)| \leq \epsilon_k \|\hat{H}^n\|, \quad (156)$$

where $\xi \in [0, t]$.

Furthermore, let us assume that $\|\hat{H}\| \geq 1$ so that $\|\hat{H}^n\| \geq \|\hat{H}^{n-1}\|$. We summarize the bounds below:

$$|h(t)| \leq E_k \leq \epsilon_k \|\hat{H}\| \leq \epsilon_k \|\hat{H}^4\|, \quad (157)$$

$$|h^{(1)}(t)| \leq V_k \leq \epsilon_k \|\hat{H}^2\| \leq \epsilon_k \|\hat{H}^4\|, \quad (158)$$

$$|h^{(2)}(t)| \leq |\langle \omega_k | \hat{H}^3 | \omega_k \rangle - E_k \langle \omega_k | \hat{H}^2 | \omega_k \rangle| \leq \epsilon_k \|\hat{H}^3\| \leq \epsilon_k \|\hat{H}^4\|, \quad (159)$$

$$|h^{(3)}(t)| \leq |\langle \omega_k | H^4 | \omega_k \rangle - \langle \omega_k | H^3 | \omega_k \rangle E_k - 3\langle \omega_k | H^3 | \omega_k \rangle E_k + 3\langle \omega_k | H^2 | \omega_k \rangle^2| \leq 4\epsilon_k \|\hat{H}^4\|. \quad (160)$$

The final term requires an additional assumption that $t\|\hat{H}\| \leq 1$. With this,

$$|(1 - e^{it})h^{(4)}(t)| \leq t|-3\langle \omega_k | H^4 | \omega_k \rangle E_k + 2\langle \omega_k | H^3 | \omega_k \rangle \langle \omega_k | H^2 | \omega_k \rangle + \langle \omega_k | H^5 | \omega_k \rangle| \quad (161)$$

$$\leq t\langle \omega_k | H^5 | \omega_k \rangle + 2t \max\{\langle \omega_k | H^4 | \omega_k \rangle E_k, \langle \omega_k | H^3 | \omega_k \rangle \langle \omega_k | H^2 | \omega_k \rangle\} \quad (162)$$

$$\leq 3t\epsilon_k \|\hat{H}^5\| \leq 3\epsilon_k \|\hat{H}^4\|. \quad (163)$$

Putting Eqn. (157)-(163) back into Eq. (155), we obtain

$$f^{(4)}(\xi) \leq 60\epsilon_k \|\hat{H}\|^4. \quad (164)$$

Plugging Eq. (164) into the choice of t as detailed after Eq. (153) concludes the proof of the theorem (recall that $t = \sqrt{s_k}$). \square

B. Exponential fidelity convergence of DB-QITE: Proof of Theorem 2

Before we begin, recall that $|\lambda_0\rangle$ denotes the ground-state. In this section, we set the reference point $\lambda_0 = 0$, i.e. the ground-state is of zero energy. Consequently, the spectral gap is given by $\Delta = \lambda_1 - \lambda_0 = \lambda_1$. With this assumption, we now present the proof of Theorem. 2 of main text.

Theorem 17. ground-state fidelity increase guarantee. Suppose that DB-QITE is initialized with some non-zero initial ground-state overlap F_0 . Let \hat{H} be a Hamiltonian with a unique ground-state $|\lambda_0\rangle$, $\lambda_0 = 0$, spectral gap Δ and spectral radius $\|\hat{H}\| \geq 1$. Let U_0 be an arbitrary unitary and set

$$s = \frac{\Delta}{12\|\hat{H}\|^3}. \quad (165)$$

The states $|\omega_k\rangle := U_k|0\rangle$, where U_k is defined in main text, i.e.

$$U_{k+1} = e^{i\sqrt{s_k}\hat{H}} U_k e^{i\sqrt{s_k}|0\rangle\langle 0|} U_k^\dagger e^{-i\sqrt{s_k}\hat{H}} U_k, \quad (166)$$

has the ground-state fidelity lower-bounded by

$$F_k := |\langle \lambda_0 | \omega_k \rangle|^2 \geq 1 - q^k \quad (167)$$

where $q = 1 - sF_0\Delta$.

Proof. From RHS of Eq. (126), the DB-QITE recursion is given by

$$|\omega_{k+1}\rangle = \left(\mathbb{1} - (1 - e^{i\sqrt{s_k}})\phi(-\sqrt{s_k})e^{i\sqrt{s_k}\hat{H}} \right) |\omega_k\rangle, \quad (168)$$

where we use the same notation again for the characteristic function (similar to Theorem. 16), i.e.

$$\phi(t) := \langle \omega_k | e^{it\hat{H}} | \omega_k \rangle. \quad (169)$$

For all subsequent calculations in this proof, we define $t = \sqrt{s_k}$ to simplify the notation. Our ultimate goal is to show that the fidelity between the ground-state and the k -th DBQA state (F_k) can be lower-bounded by

$$F_k \geq 1 - q^k, \quad (170)$$

where q is a real parameter such that $0 < q < 1$. To do so, we define the ground-state infidelity $\epsilon_k := 1 - F_k$ and we will derive a recursive inequality relating ϵ_k and ϵ_{k+1} .

First, let us define the overlap between the ground-state and the k -th DBQA state as $\langle \lambda_0 | \omega_k \rangle$, which is related to the fidelity F_k by $F_k = |\langle \lambda_0 | \omega_k \rangle|^2$. Using Eq. (168), the overlap at $(k+1)$ -th and k -th DBQA recursion is related by

$$\langle \lambda_0 | \omega_{k+1} \rangle = \langle \lambda_0 | \omega_k \rangle - (1 - e^{it})\phi(-t)\langle \lambda_0 | e^{it\hat{H}} | \omega_k \rangle \quad (171)$$

$$= (1 - (1 - e^{it})\phi(-t)) \langle \lambda_0 | \omega_k \rangle, \quad (172)$$

where we use the expression $\langle \lambda_0 | e^{it\hat{H}} = \langle \lambda_0 | e^{it\lambda_0}$ and the assumption $\lambda_0 = 0$ in the last line. Using Eq. (172), the ground-state fidelities F_{k+1} and F_k are related by

$$F_{k+1} = |\langle \lambda_0 | \omega_{k+1} \rangle|^2 = |g(t)|^2 F_k, \quad (173)$$

where we define $g(t) = 1 - (1 - e^{it})\phi(-t)$. Using the definition of the infidelities, the ground-state infidelities ϵ_k and ϵ_{k+1} are related by

$$\epsilon_{k+1} = 1 - |g(t)|^2(1 - \epsilon_k) = \epsilon_k - p(t)(1 - \epsilon_k). \quad (174)$$

where we also define $p(t) = |g(t)|^2 - 1$ for simplicity. Now, the remaining task is to show that $p(t) \geq c\epsilon_k$ for some positive constant c . We start by applying Taylor's theorem (see Sec. I), i.e.

$$p(t) = p(0) + tp^{(1)}(0) + \frac{t^2}{2}p^{(2)}(0) + \frac{t^3}{6}p^{(3)}(0) + \frac{t^4}{24}p^{(4)}(\xi), \quad (175)$$

where $\xi \in [0, t]$. Notice that $p(t)$ is an even function with $p(0) = 0$ as

$$p(-t) = |g(-t)|^2 - 1 = |g(t)^*|^2 - 1 = |g(t)|^2 - 1 = p(t), \quad (176)$$

Hence, all odd order derivatives of $p(t)$ vanish, i.e. $p^{(2n+1)}(0) = 0$ for any non-negative integer n . Therefore, the Taylor series reduces to

$$p(t) = \frac{t^2}{2}p^{(2)}(0) + \frac{t^4}{24}p^{(4)}(\xi). \quad (177)$$

1. Directly evaluating $p^{(2)}(t)$ yields

$$p^{(2)}(t) = 2\text{Re}[g^*(t)g^{(2)}(t)] + 2|g^{(1)}(t)|^2, \quad (178)$$

To determine the expression of the term $p^{(2)}(0)$, we explicitly compute the derivatives of $g(t)$ up to second order. The results are given by

$$g^{(1)}(t) = ie^{it}\phi(-t) + (1 - e^{it})\phi^{(1)}(-t), \quad (179)$$

$$g^{(2)}(t) = -e^{it}\phi(-t) - 2ie^{it}\phi^{(1)}(-t) - (1 - e^{it})\phi^{(2)}(-t). \quad (180)$$

Thus, we obtain

$$p^{(2)}(0) = 2\text{Re}[g^*(0)g^{(2)}(0)] + 2|g^{(1)}(0)|^2 \quad (181)$$

$$= 2\text{Re}[1 \cdot (-1 + 2E_k)] + 2|i|^2 = 4E_k. \quad (182)$$

where we use the relation $g^{(1)}(0) = i$, $\phi(0) = 1$ and $\phi^{(1)}(0) = iE_k$.

2. Here, we will derive an lower bound for the term $p^{(4)}(\xi)$.

First, recall that $p(t) = g(t)g^*(t) - 1$ and hence its n -th order derivative is given by

$$p^{(n)}(t) = \sum_{\substack{n_a, n_b = 1, \\ n_a + n_b = n}}^n g^{(n_a)}(t)g^{*(n_b)}(t), \quad (183)$$

where the constraint $n_a + n_b = n$ arises from the Leibniz rule. We can collect identical terms and rewrite it as

$$p^{(n)}(t) = \sum_{r=0}^n \binom{n}{r} g^{(r)}(t)g^{*(n-r)}(t), \quad (184)$$

where we introduce the factor $\binom{n}{r}$ to account for combinatorial degeneracy. In particular, for $n = 4$, we have

$$p^{(4)}(t) = g(t)g^{*(4)}(t) + 4g^{(1)}(t)g^{*(3)}(t) + 6g^{(2)}(t)g^{*(2)}(t) + 4g^{(3)}(t)g^{*(1)}(t) + g^{(4)}(t)g^*(t). \quad (185)$$

To obtain the lower bound for $p^{(4)}(\xi)$, we first derive an upper bound for $|g^{(r)}(\xi)|$ with arbitrary non-negative integer r .

(a) In this part, we will determine the upper bound for $|g(\xi)|$.

Recall that $g(t) = 1 - (1 - e^{it})\phi(-t)$ and we define $a(t) = -(1 - e^{it})$ for notational simplicity. For the factor $a(\xi)$, it gives

$$|a(\xi)| = |1 - e^{i\xi}| = \sqrt{(1 - \cos \xi)^2 + \sin^2 \xi} = \sqrt{2 - 2\cos \xi} = \sqrt{4\sin^2 \frac{\xi}{2}} \leq 2 \left| \sin \frac{\xi}{2} \right| \leq \xi, \quad (186)$$

where we use the trigonometric identities $\cos \xi = 1 - 2\sin^2 \frac{\xi}{2}$ in the last equality and we use the relation $|\sin \frac{\xi}{2}| \leq \frac{\xi}{2}$ in the last inequality. Thus, we have

$$|g(\xi)| \leq 1 + |a(\xi)||\phi(-\xi)| \leq 1 + \xi \leq 2, \quad (187)$$

where we use the triangle inequality in the first inequality and we use the bound $|\phi(-\xi)| \leq 1$. Note that $\xi \leq t \leq 1$ by assumption.

(b) Next, we compute the upper bound for $|g^{(r)}(\xi)|$. For r -th order derivatives of $g(t)$, we have

$$|g^{(r)}(\xi)| = \left| \sum_{m=0}^r \binom{r}{m} a^{(m)}(\xi)\phi^{(r-m)}(-\xi) \right| \leq \sum_{m=0}^r \binom{r}{m} |a^{(m)}(\xi)| |\phi^{(r-m)}(-\xi)|, \quad (188)$$

where we use a similar procedure from Eq. (184) to deal with the combinatorial degeneracy. We then split the sum into $m = 0$ case and $m \neq 0$ cases to evaluate the upper bound, i.e. it becomes

$$|g^{(r)}(\xi)| \leq |a(\xi)| |\phi^{(r)}(-\xi)| + \sum_{m=1}^r \binom{r}{m} |a^{(m)}(\xi)| |\phi^{(r-m)}(-\xi)| \quad (189)$$

$$\leq \xi \epsilon_k \|\hat{H}\|^r + \sum_{m=1}^r \binom{r}{m} \epsilon_k \|\hat{H}\|^{r-m}. \quad (190)$$

For the first term, we use the bound $|a(\xi)| \leq \xi$ (Eq. (186)) and Eq. (133). Similarly, for the second term, we use the bound $|a^{(m)}(\xi)| \leq 1$ and Eq. (133). Furthermore, let us assume that $1 \leq \|\hat{H}\|$ which leads to $\|\hat{H}^r\| \geq \|\hat{H}^{r-1}\|$. Thus, it simplifies to

$$|g^{(r)}(\xi)| \leq \epsilon_k \|\hat{H}\|^{r-1} + \sum_{m=1}^r \binom{r}{m} \epsilon_k \|\hat{H}\|^{r-1} = \epsilon_k \|\hat{H}\|^{r-1} \left(1 + \sum_{m=1}^r \binom{r}{m} \right) \quad (191)$$

$$= 2^r \epsilon_k \|\hat{H}\|^{r-1}. \quad (192)$$

where we assume that $\xi \|\hat{H}\| \leq 1$ in the first inequality and we employ binomial identity in the last inequality.

Finally, observe that Eq. (185) can be upper-bounded by

$$|p^{(4)}(\xi)| \leq 2|g(\xi)| \times |g^{(4)}(\xi)| + 8|g^{(1)}(\xi)| \times |g^{(3)}(\xi)| + 6|g^{(2)}(\xi)|^2, \quad (193)$$

where we use the fact that $|g^{(r)}(\xi)| = |g^{*(r)}(\xi)|$. Using Eq. (187) and Eq. (192), it becomes

$$|p^{(4)}(\xi)| \leq 64\epsilon_k \|\hat{H}\|^3 + 128\epsilon_k^2 \|\hat{H}\|^2 + 96\epsilon_k^2 \|\hat{H}\|^2 \quad (194)$$

$$\leq 64\epsilon_k \|\hat{H}\|^3 + 128\epsilon_k \|\hat{H}\|^3 + 96\epsilon_k \|\hat{H}\|^3 = 288\epsilon_k \|\hat{H}\|^3, \quad (195)$$

where we use the bounds $\epsilon_k^2 \leq \epsilon_k$ and $|\hat{H}|^2 \leq \|\hat{H}\|^3$ in the last line. Finally, the lower bound for $p^{(4)}(\xi)$ is given by

$$|p^{(4)}(\xi)| \leq 288\epsilon_k \|\hat{H}\|^3 \implies p^{(4)}(\xi) \geq -288\epsilon_k \|\hat{H}\|^3. \quad (196)$$

Combining Eq. (177), Eq. (182) and Eq. (196) yields

$$p(t) \geq 2t^2 E_k - 12t^4 \epsilon_k \|\hat{H}\|^3 \quad (197)$$

$$\geq 2t^2 \Delta \epsilon_k - 12t^4 \epsilon_k \|\hat{H}\|^3, \quad (198)$$

where we use the bound $E_k \geq \lambda_1 \epsilon_k = \Delta \epsilon_k$ as shown in Lemma. 3. As stated in Theorem. 2, we set $t^2 = s = \frac{\Delta}{12\|\hat{H}\|^3}$ as a constant for all k -th DB-QITE recursions. Thus, $p(t)$ can be lower-bounded by

$$p(t) \geq 2\epsilon_k \left(\frac{\Delta^2}{12\|\hat{H}\|^3} - \frac{6\Delta^2}{144\|\hat{H}\|^3} \right) = \frac{\Delta^2 \epsilon_k}{12\|\hat{H}\|^3}. \quad (199)$$

Substituting it into Eq. (174) yields

$$\epsilon_{k+1} \leq \epsilon_k - (1 - \epsilon_k) \frac{\Delta^2 \epsilon_k}{12\|\hat{H}\|^3} = \left(1 - \frac{\Delta^2 F_k}{12\|\hat{H}\|^3} \right) \epsilon_k \leq \left(1 - \frac{\Delta^2 F_0}{12\|\hat{H}\|^3} \right) \epsilon_k = q \epsilon_k, \quad (200)$$

where $q = 1 - s F_0 \Delta$ as mentioned in Theorem. 2. Ultimately, the ground-state fidelity is given by

$$\epsilon_k \leq q^k \epsilon_0 \implies F_k \geq 1 - q^k F_0 \geq 1 - q^k \quad (201)$$

where we used that $\epsilon_0 = 1 - F_0 \leq 1$.

□

C. Runtime consideration

We remark that Eq. (177) implies the relation $F_{k+1} = F_k + 2E_k s + \mathcal{O}(s^2)$ stated as Eq. (25) above. Next, we provide a calculation of the depth in DB-QITE in the weaker setting of choosing s via Eq. (15), so independent of encountered energy E_k or energy variance V_k .

Corollary 18. *For L qubits, DB-QITE amplifies initial fidelity F_0 to desired fidelity F_{th} in circuit depth*

$$\mathcal{O}\left(L\left(\frac{1-F_0}{1-F_{th}}\right)^{2/(sF_0\Delta)}\right). \quad (202)$$

where $s = \frac{\Delta}{12\|\hat{H}\|^3}$ as defined in Theorem. 2.

Proof. We use Eq. (201) to find k such that

$$\epsilon_k \leq q^k \epsilon_0 \leq \epsilon_{th} := 1 - F_{th}. \quad (203)$$

After taking the logarithm on both sides we define

$$k = \lceil \log(\epsilon_{th}/\epsilon_0) / \log(q) \rceil. \quad (204)$$

Finally, we insert the lower bound to the query complexity estimate

$$\mathcal{O}(3^k) = \mathcal{O}\left((\epsilon_{th}/\epsilon_0)^{\log(3)/\log(q)}\right) \quad (205)$$

$$= \mathcal{O}\left((\epsilon_{th}/\epsilon_0)^{\log(3)/\log(1-sF_0\Delta)}\right) \quad (206)$$

$$= \mathcal{O}\left((\epsilon_0/\epsilon_{th})^{\log(3)/(sF_0\Delta)}\right), \quad (207)$$

where we use the identity $a^{\log_x(b)} = b^{\log_x(a)}$ in the first line and $\log(1-x) \approx -x$ in the last line. We bound the depth of each subroutine query as $\mathcal{O}(L)$ (i.e. dominated by reflections [95, 97] as opposed to Hamiltonian simulations which can be done in $\mathcal{O}(1)$ time) so the overall depth is as stated. \square

V. Numerical simulations and gate-counts of DB-QITE using Qrisp

In this section, we provide numerical simulations and gate-counts for the compiled circuits for DB-QITE. A fully compilable implementation of DB-QITE requires careful management of quantum-algorithmic primitives. We utilize the Qrisp programming framework [104], whose automated memory management handles the exchange of auxiliary qubits across different modules without complicating the code. Simulations are performed using Qrisp's integrated *statevector* simulator that leverages sparse matrices, enabling the simulation of DB-QITE for relatively large quantum systems. Apart from that, the simulator efficiently checks for potential factorization of state vectors, which can reduce the required resources significantly.

A. Compilation for DB-QITE

Our implementation utilizes the compilation primitives available within Qrisp to realize the DB-QITE unitary defined recursively in Eq. (13). The DB-QITE unitary involves Hamiltonian evolutions and reflection gates, both of which need to be decomposed into the CZ + U3 gate set for execution on available quantum hardware, and Clifford + T gate set for execution on fault-tolerant quantum hardware. Hamiltonian evolutions ($e^{i\sqrt{t}\hat{H}}$) are implemented using Trotter-Suzuki decomposition [93]. This is the standard approach to the task of Hamiltonian simulation and yields an efficient implementation when scaling the evolution duration. For the two-local Hamiltonians considered in our numerical studies, each term in the Trotter expansion can be efficiently simulated using a small number of CZ and single qubit rotations U3. To optimize the simulation depth, Qrisp's native implementation of Trotter-Suzuki decomposition employs a heuristic graph-coloring algorithm [139] to parallelize the execution of Hamiltonian terms acting on non-overlapping qubits.

The reflection unitary is a multi-qubit controlled parameterized phase gate, assuming the quantum state is the tensor-product zero state; we see it by writing $e^{i\sqrt{t}|0\rangle\langle 0|} = \mathbb{1} + (e^{i\sqrt{t}} - 1)|0\rangle\langle 0|$ with matrix representation

$$e^{i\sqrt{t}|0\rangle\langle 0|} = \begin{bmatrix} e^{i\sqrt{t}} & 0 & 0 & 0 \\ 0 & 1 & 0 & 0 \\ 0 & 0 & \ddots & 0 \\ 0 & 0 & 0 & 1 \end{bmatrix}. \quad (208)$$

This means that the first qubit is the target to which the operation $\text{diag}(e^{i\sqrt{t}}, 1)$ is applied, and the remaining $L - 1$ qubits are the control qubits.

Qrisp's native compilation routine for implementing the reflection gates ($e^{i\sqrt{t}|0\rangle\langle 0|}$) is based on Ref. [96]. The Qrisp implementation however deviates from the original implementation in a crucial way: The intermediate control values are no longer uncomputed via Margolus gates [140] but instead Gidney's temporary logical AND [141]. This reduces the CZ count of the uncomputation from 3 to 0.5 (the CZ count only needs to be performed in half of the cases) and the T count from 4 to 0.

The above described technique is suitable to implement a multi-controlled X gate, the algorithm requires a multi-controlled phase gate. In principle, this can be achieved by wrapping two MCX gates around a phase gate and an ancilla. However, there is an even better way to achieve this. For this notice, that Balaucá's MCX is a conjugation, i.e. of the form

$$MCX = VWV^\dagger. \quad (209)$$

The V operator (un)computes the ancilla value, whilst the W operator performs a simple Toffoli gate. We modify this structure in the following way towards implementing a multi-controlled phase gate:

$$MCP(\Phi) = (VW)P(\Phi)(VW)^\dagger. \quad (210)$$

In words: We use Balaucá's ancillae computation method to reduce the control value into a single ancilla qubit, which is in the $|1\rangle$ state if the required conditional is given. On this ancilla, we execute the phase gate and conclude with the uncomputation of all involved ancillae.

A recently published, viable alternative is the compilation of multi-controlled X-gates using conditionally clean ancillae (CCA) [142]. This method exhibits a similar conjugation structure, but in this case the W operator requires a constant number of ancillae. The same technique as above can be used to implement a multi-controlled phase gate. The resulting procedure requires less ancillae, but it cannot use Gidney's logical AND for uncomputation. This fact drives the T-cost ($8n - 13$ for CCA and $4n - 1$ for Balaucá). As discussed in [141], blocking an ancilla qubit for a given amount of space-time gives rise to an opportunity cost in the T count because the blocked ancillae cannot be used for T-state production. However, this cost is highly dependent on the space-time volume required to produce T states, which might change significantly until fault-tolerant quantum devices become available. The answer to the question which of these options proves advantageous therefore stays open.

For numerical simulations we utilize the latter procedure as it requires only a constant number of ancillae and handling a smaller amount of qubits is helpful for simulations.

B. Numerical simulations of the Heisenberg model and initial states

Let us consider DB-QITE applied to the antiferromagnetic Heisenberg model

$$\hat{H} = \sum_{i=1}^{L-1} (X_i X_{i+1} + Y_i Y_{i+1} + Z_i Z_{i+1}) \quad (211)$$

where L is the number of qubits. For the numerical simulations, we consider $L \in \{10, 12, 14, 16, 18, 20\}$. Hamiltonian simulation, i.e. the unitary $e^{i\tau H}$, is implemented via the second-order Trotter-Suzuki formula with 2 steps. We remark that for some cases, one layer of the second-order Trotter-Suzuki formula could suffice. In terms of runtime, roughly, each layer has linear runtime just like the reflection unitaries. In each step, we perform 2 Hamiltonian simulations and 1 reflection unitary; hence, taking 1 rather than 2 layers of the Trotter-Suzuki formula would lead to a shorter runtime, while in cases where K layers are required, the runtimes presented below will scale in proportion to K .

In every DB-QITE step, we use a 20-point grid search to find the s_k that yields the best energy gain. Additionally, Eq. (9) has an approximate invariance

$$G_{\alpha\beta s}(\hat{A}/\alpha, \hat{B}/\beta) = e^{i\sqrt{s\beta/\alpha}\hat{A}} e^{i\sqrt{s\alpha/\beta}\hat{B}} e^{-i\sqrt{s\beta/\alpha}\hat{A}} e^{-i\sqrt{s\alpha/\beta}\hat{B}} = e^{-s[\hat{A}, \hat{B}]} + \mathcal{O}(s^{3/2}), \quad (212)$$

but rescaling by α, β can influence the approximation constant in $\mathcal{O}(s^{3/2})$ [32]. Specifically, we have

$$\|G_{\alpha\beta s}(\hat{A}/\alpha, \hat{B}/\beta) - e^{-s[\hat{A}, \hat{B}]} \| \leq s^{3/2}(\|[\hat{A}, [\hat{A}, \hat{B}]]\|/\sqrt{\beta/\alpha} + \|[\hat{B}, [\hat{A}, \hat{B}]]\|/\sqrt{\alpha/\beta}). \quad (213)$$

We found empirically that setting $\alpha = 10$ and $\beta = 1$ allows us to identify time steps s_k that yield better ground-state approximations than those obtained without reweighting the contributions of \hat{H} and ω_k .

We further remark that the DB-QITE steps involve two Hamiltonian simulations and one reflection. Depending on which of these components is more robust under noise, reweighting can be adjusted to improve noise resilience. For instance, by shortening the Hamiltonian simulation time and thus using fewer Trotter-Suzuki layers. When optimizing for noise robustness or shorter circuits, the optimal reweighting strategy may differ from the one we used, which was designed to maximize energy decrease per step rather than circuit robustness.

Next, we discuss two types of initial states which *a)* are designed analytically based on physical intuition so should remain meaningful for larger systems and *b)* we consider a variational circuit which improves the initialization quality but may not be scalable. Specifically, we consider *a)* a tensor product of singlet states

$$|\text{Singlet}\rangle = 2^{-L/4}(|10\rangle - |01\rangle)^{\otimes L/2} \quad (214)$$

of consecutive qubits, and *b)* a type of the so-called problem-specific Hamiltonian Variational Ansatz (HVA) [98–100]

$$|\text{HVA}_p(\mathbf{t})\rangle = \prod_{j=1}^p (e^{-it_{j,0}\hat{H}_0} e^{-it_{j,1}\hat{H}_1}) |\text{Singlet}\rangle \quad (215)$$

where \hat{H}_0, \hat{H}_1 are obtained from \hat{H} by restricting to summation over odd (even) indices i such that all terms in \hat{H}_0, \hat{H}_1 commute. In numerics, we will use just one layer $p = 1$ because it will be enough to illustrate the case of a significant improvement of the initialization. In other words we use the ansatz

$$|\text{HVA}\rangle = e^{-it_0\hat{H}_0} e^{-it_1\hat{H}_1} |\text{Singlet}\rangle = U_{\text{HVA}} |\text{Singlet}\rangle \quad (216)$$

whose meaning is to balance between the location of the singlets and putting the singlet sublattices into a superposition.

Fig. 3 shows the performance of DB-QITE for a range of system sizes $L = 10, 12, \dots, 20$ for both these initial conditions. For all L , we find that just $k = 2$ DB-QITE steps allow to reach 90% fidelity when initializing with HVA. We find across all considered system sizes that a better quality of initialization leads to a better DB-QITE performance, both in terms of ground-state fidelity and achieved energy. However, for $L = 20$ (which requires decreasing the Qrisp simulator's sparsity cut-off ratio to ensure high precision simulations) we find that the convergence requires more than $k = 5$ steps to reach an ultra-high fidelity regime, i.e. to reach fidelity exceeding $F_k \geq 99\%$ in that many-body system. Having said that even for $L = 20$, DB-QITE is able to prepare a state with energy within a fraction of the spectral gap Δ from the ground-state value λ_0 . This suggests that very short circuits could be enough to prepare states allowing to prepare very low-energy states for further physics studies on a quantum computer.

Fig. 4 quantifies the runtime by counting gates of the DB-QITE circuits. In near-term, the number of CZ gates matters most because usually operations on individual qubits are more coherent than gates acting on two qubits by coupling them. On the other hand, for typical error-correction codes CZ gates can be implemented transversally which makes them cheaper than some of single-qubit rotations U3 which required T -gate resources. Typically the single-qubit count is about twice the CZ count. For example, $k = 2$ for $L = 10$ leads to $F_2 \approx 99\%$ and requires $N_{\text{CZ}} \approx 1.4 \times 10^3$ CZ gates and $N_{\text{U3}} \approx 2.3 \times 10^3$ single-qubit gates. For $L = 20$ we obtain $F_2 \approx 92\%$ which requires $N_{\text{CZ}} \approx 3 \times 10^3$ CZ gates and $N_{\text{U3}} \approx 4.8 \times 10^3$ single-qubit gates. Thus, the gate cost to achieve a high ground-state fidelity qualitatively doubled when doubling the system size, while it requires a much larger effort to prepare an ultra-high fidelity ground-state approximation for the larger system.

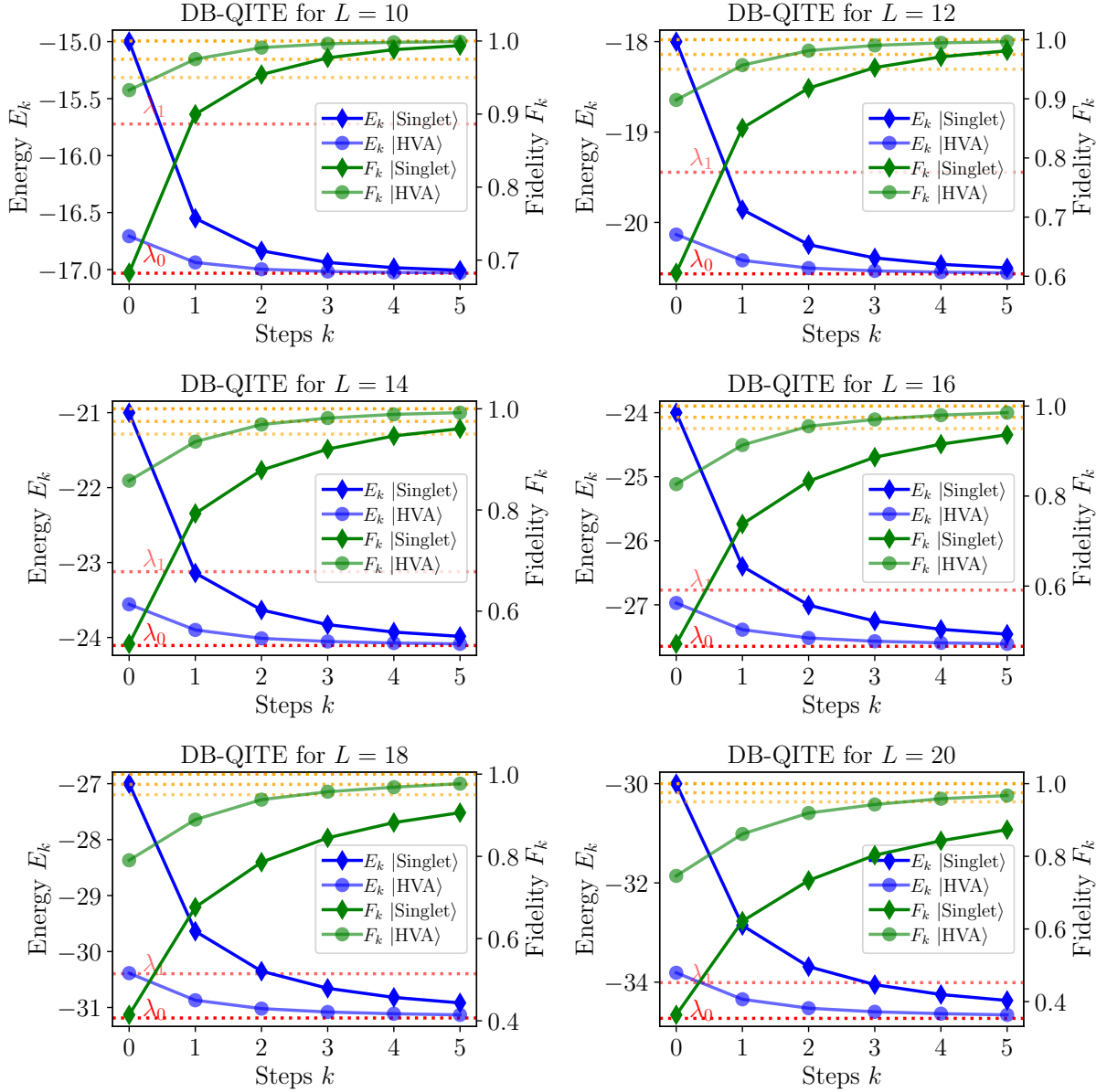


FIG. 3. 5 iterations of DB-QITE for L -qubit Heisenberg model. The figures show the energies $E_k = \langle \omega_k | \hat{H} | \omega_k \rangle$ and the fidelities $F_k = |\langle \omega_k | \lambda_0 \rangle|^2$ with the ground state $|\lambda_0\rangle$ for the k -th iterates $|\omega_k\rangle$ for initializations $|\omega_0\rangle = |\text{Singlet}\rangle$ and $|\omega_0\rangle = |\text{HVA}\rangle$. The upper (dashed, orange) lines indicate the fidelities 1.0, 0.975, 0.95, and the lower (dashed, red) lines indicate the ground state energies λ_0 and the first excited state energies λ_1 . Let us make the following observations: 1) The $|\text{HVA}\rangle$ initializations achieve a higher fidelity to the ground state compared to the $|\text{Singlet}\rangle$ initializations, and the fidelity of the k -th iterates for $|\text{HVA}\rangle$ consistently exceeds the respective fidelities for $|\text{Singlet}\rangle$. However, this gap narrows significantly for an increasing number of DB-QITE steps k . Therefore, the choice of the particular initial state can be less impactful as long as there is *some* overlap with the ground state. 2) The optimal evolution times s_k found iteratively by a 20-point grid search tend to decrease with k , while remaining orders of magnitude larger than guaranteed by Theorem 2. In particular, large initial evolution times s_0 yield a rapid decrease in energy in the first step of DB-QITE. Similarly, we observe that the reached fidelities F_k are much larger than guaranteed by Theorem 2 by optimizing the s_k durations [54]. For example, for $L = 10$ we empirically observe $F_k > 1 - q^k$ for $q = 0.5$, while Theorem 2 would merely provide a theoretical lower bound with q being close to 1. 3) The fidelity F_k with the ground state $|\lambda_0\rangle$ reached for the k -th iterate decreases with increasing number of qubits L , e.g., for 5 steps of DB-QITE with $|\text{HVA}\rangle$ initialization, fidelities $F_5 = 0.999$ for $L = 10$, and $F_5 = 0.967$ for $L = 20$ are achieved.

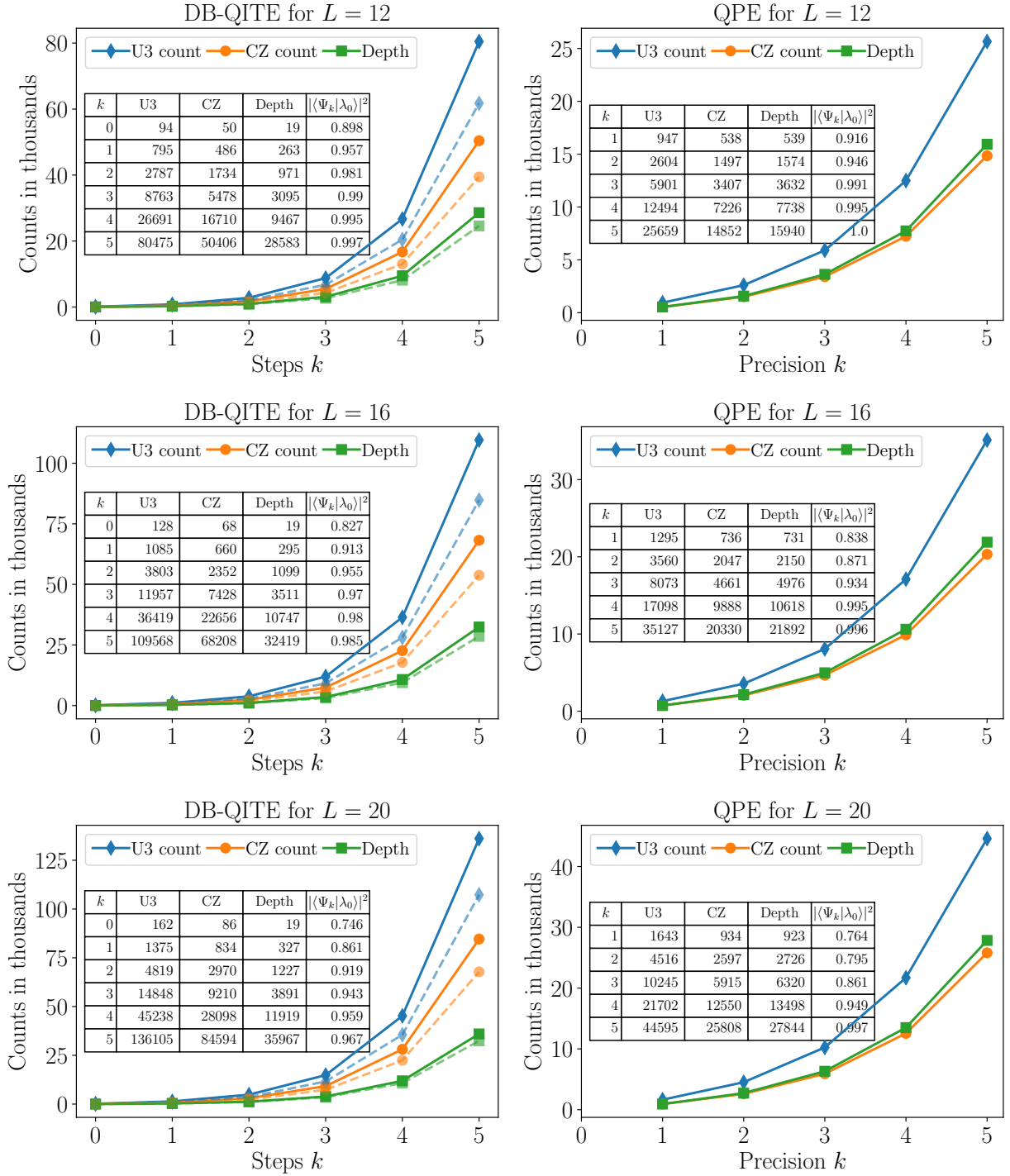


FIG. 4. Gate counts, circuit depth and ground-state fidelity for DB-QITE (left column) and QPE (right column) for the Heisenberg model with $L = 12, 16$ and 20 qubits for $|\text{HVA}\rangle$ and $|\text{Singlet}\rangle$ (dashed) as initializations. For $L = 12$ the ground state is prepared with fidelity $F_3 = 99\%$ with $k = 3$ steps of DB-QITE. The circuit implementing this requires $N_{\text{CZ}} \approx 5.5 \times 10^3$ CZ gates and $N_{\text{U3}} \approx 8.8 \times 10^3$ single-qubit gates. For $L = 20$ the ground state is prepared with fidelity $F_2 = 92\%$ with $k = 2$ steps of DB-QITE. The circuit implementing this requires $N_{\text{CZ}} \approx 3 \times 10^3$ CZ gates and $N_{\text{U3}} \approx 4.8 \times 10^3$ single-qubit gates. The structure of DB-QITE's circuits is more homogeneous and e.g. for $k = 4$ DB-QITE has circuit depth $D_4 \approx 1.2 \times 10^4$ reaching $F_4 \approx 96\%$ which is lower circuit depth of QPE with $k = 4$ precision qubits given by $D_4 \approx 1.3 \times 10^4$ giving only $F_4 \approx 95\%$. When considering long enough circuits then QPE reaches enough precision (k for QPE denotes the number of auxiliary qubits encoding precision) and under the assumption of all-to-all connectivity outperforms DB-QITE by reaching higher fidelity through less gates and lower circuit depth.

C. Conditions for quantum phase estimation (QPE) to outperform DB-QITE

We next compare the runtime of DB-QITE to that of quantum phase estimation (QPE) for the ground-state preparation task. Specifically, we will make a comparison to ground state preparation with phase estimation for known ground energy reviewed in Ref. [21]. We here aim to compare to the (likely) strongest algorithmic method in the regime when classical simulation is available. In other words, for $L \leq 20$ qubits we can compute almost all relevant quantities to tightly parametrize QPE by having a $[0, 1)$ spectrum. In the case of $L \gg 20$ qubits such classical aid will not be present for a general Hamiltonian and we discuss the prospective runtime overheads later in this section and next introduce the precise method.

a. Description of the procedure for QPE. To set up the method we apply an affine transformation $\hat{H} \mapsto \hat{H}' = (\hat{H} - \lambda_0 \mathbb{1})/(\|\hat{H}\| - \lambda_0)$ to achieve that $\lambda_0 = 0$ and the spectrum of \hat{H} is contained in $[0, 1)$. We then perform controlled-evolutions using the rescaled Hamiltonian $U_j = \Lambda_j(e^{2\pi i 2^j \hat{H}'})$ where Λ_j indicates controlling on qubit j . The label j encodes the digit of precision accessed. The protocol then concludes by performing a measurement on all of the k qubits encoding the precision and given the rescaling to $[0, 1)$ the ground-state will correspond to measuring 0's. Hamiltonian simulation, i.e. the unitary e^{itH} , is implemented via the second-order Trotter formula with 2 steps for both methods. The control Λ_j is implemented by standard compilation methods which are natively available in Qrisp. The success probability of preparing the (exact) ground state with QPE is upper bounded by the fidelity $F_0 = |\langle \omega_0 | \lambda_0 \rangle|^2$ of the initial state with the ground state.

b. QPE vs. DB-QITE for singlet initialization. Fig. 5 summarizes the results for the $|\text{Singlet}\rangle$ initial condition. First, for DB-QITE we find a gradual increase of recursion steps required to reach a threshold fidelity. Second, the gate count is exponential in the number of steps.

For $L = 10$, DB-QITE with $k = 2$ steps provides ground-state fidelity $F_2 \approx 95\%$ requiring $N_{\text{CZ}} \approx 1.1 \times 10^3$ CZ gates and $N_{\text{sq}} \approx 1.7 \times 10^3$ single-qubit gates. QPE with $k = 2$ precision qubits provides ground-state fidelity $F_2 \approx 92\%$ with a success probability of $P \approx 76\%$ requiring $N_{\text{CZ}} \approx 1.2 \times 10^3$ CZ gates and $N_{\text{sq}} \approx 2.1 \times 10^3$ single-qubit gates lagging the results for DB-QITE. Importantly, $k = 2$ requires about a thousand two-qubit gates which is within the reach of commercially available quantum hardware.

When aiming for higher fidelities, QPE starts to outperform DB-QITE: For $L = 10$, DB-QITE with $k = 3$ steps provides ground-state fidelity $F_3 \approx 98\%$ requiring $N_{\text{CZ}} \approx 3.5 \times 10^3$ CZ gates and $N_{\text{sq}} \approx 5.5 \times 10^3$ single-qubit gates. QPE with $k = 3$ precision qubits provides ground-state fidelity $F_3 \approx 100\%$ with a success probability of $P \approx 70\%$ requiring $N_{\text{CZ}} \approx 2.7 \times 10^3$ CZ gates and $N_{\text{sq}} \approx 4.7 \times 10^3$ single-qubit gates.

With increasing number of qubits L , and decreasing initial fidelity F_0 , the comparison further shifts in favor of QPE: For $L = 20$, QPE with $k = 5$ precision qubits provides ground-state fidelity $F_5 \approx 99\%$ with a success probability of $P \approx 37\%$ requiring $N_{\text{CZ}} \approx 2.6 \times 10^5$ CZ gates and $N_{\text{sq}} \approx 4.4 \times 10^5$ single-qubit gates. For DB-QITE the fidelity F_5 remains well below 90%. Unfortunately it is unrealistic to expect that this performance of QPE compared to DB-QITE would be sustained in cases when the ground-state energy is not known exactly. In that case the spectrum would not be scaled as tightly and QPE would require more precision qubits and thus a much larger runtime. See Ref. [21] for analytical estimates of the overheads in the case where λ_0 is not known.

c. QPE vs. DB-QITE for inaccurate spectrum rescaling. In addition to results of QPE applied with the Hamiltonian \hat{H}' rescaled to the $[0, 1)$ interval, Fig. 5 presents results for $\hat{H}'/2$ rescaled to $[0, 1/2)$ and $\hat{H}'/10$ rescaled to $[0, 1/10)$. This models a situation where QPE receives a strong guidance about the ground-state energy λ_0 but the norm $\|\hat{H}\|$ is over-estimated by a factor of 2 and 10, respectively. Such over-estimation could arise, e.g. from using the triangle inequality for a decomposition of \hat{H} into a sum of terms whose norm is known. For example, for the Heisenberg model we have

$$\|\hat{H}\| \leq \sum_{i=1}^{L-1} \|X_i X_{i+1} + Y_i Y_{i+1} + Z_i Z_{i+1}\| \leq \sum_{i=1}^{L-1} (\|X_i X_{i+1}\| + \|Y_i Y_{i+1}\| + \|Z_i Z_{i+1}\|) \leq 3(L-1) \quad (217)$$

which would give $\|\hat{H}\| \leq 57$ for $L = 20$ which is very loose but represents a difficulty that would appear for use-cases of quantum computation for difficult optimization instances in materials science. We find that if one knows the exact values of λ_0 and $\|\hat{H}\|$ then QPE outperforms DB-QITE on platforms which have all-to-all interactions. Thus, QPE requires stronger assumptions compared to DB-QITE and in near-term the latter will be advantageous.

We stress that the rescaling will be even worse when λ_0 is not known exactly. Then the spectrum will not be rooted at 0 and thus even more qubits will be required to resolve the energy with sufficient precision. Moreover, the precise value of the ground-state energy will not be known and given that the initial ground-state fidelity may not be known then QPE might need to be executed for very many instances in order to allocate sufficient probability of observing measurement corresponding to the ground-state.

This should be compared with DB-QITE which is a quantum algorithm of a different type and thus requires no such estimates. Our numerical results are computed based on evaluations of E_k for 20 different values of s_k . On quantum hardware this would require estimation of E_k from data which is a well-studied problem and can be expected to be relatively robust (e.g. in comparison to evaluating gradients of E_k with respect to microscopic parameters of the circuit as opposed to the macro-parameter s_k). The

overhead for the estimation E_k will scale with k and given that k must be kept at minimum it should not affect the runtime substantially.

d. QPE vs. DB-QITE for pretrained initializations. These observations remain in place also for the variational initializations $|\text{HVA}\rangle$ presented in Fig. 5. Again, if exact rescaling is in place then QPE outperforms DB-QITE in reaching the ultra-high fidelity $F_5 \geq 99\%$. On the other hand, we see that DB-QITE benefits from an improved initialization more than QPE. Specifically, for $L = 20$ both DB-QITE with $k = 3$ steps and QPE with $k = 4$ precision qubits reach a fidelity of about 95% through a similar runtime. We remark that the steps are different in nature for these methods but they qualitatively coincide because for each there is a notion of exponential convergence at play. To reach fidelity $F_2 \geq 90\%$ DB-QITE is the preferred method because $k = 2$ steps suffice while for $k = 2$ QPE has $F_2 \ll 90\%$ and so DB-QITE has significantly faster runtime to reach the threshold of 90% fidelity than QPE.

Finally, we comment that the circuit used to pretrain the initialization is a generalization of the $|\text{Singlet}\rangle$ initial state because it uses Hamiltonian evolutions that rotate towards singlets on alternating even and odd sublattices while $|\text{Singlet}\rangle$ implements them on only one sublattices. However, despite the clear advantage of being informed by the physics of the model, the ansatz we use for training is limited in expressivity as it uses a low-depth circuit. This showcases the strength of DB-QITE whose operation through quantum computation implements the intuition about the physics of the system in that DB-QITE implements steps along the Riemannian gradient which reduces the energy cost-function.

e. Discussion of susceptibility to noise. Finally, we comment in more detail about the robustness to experimental noise on near-term hardware.

Firstly, on architectures which do not have all-to-all interactions the runtime of both methods will be increase, generally DB-QITE should be less affected. Specifically, the native connectivity must be used to route using SWAP gates connections needed for the required non-local gates [143–145]. Ref. [97] shows that the reflection gates can be compiled with linear scaling and the proportionality constant increases only slightly even if the hardware architecture has only nearest-neighbour connectivity. There is a difference, however, in that QPE needs routing from the qubits encoding the system to the qubits encoding the digits of the energy read-out. This difference will show up especially in cases when the connectivity of the input Hamiltonian matches the hardware architecture. In that case, Hamiltonian simulation in DB-QITE will have no routing overheads while the controlled Hamiltonian simulation of QPE will require it. Additionally, with the constructions in Ref. [142], the reflections can be executed with nearest-neighbor gates in linear time.

Besides overheads, the methods differ in their reliance on two-qubit gates. For QPE the reliance is fundamental and the qubits responsible for precision will not faithfully represent the energy of the system if the controlled unitary operations are not close enough to perfection. This could lead to measurements that point to wrong bits showing up in the energy representation. In turn, for DB-QITE miscalibration of gates has a relatively transparent outcome: Two-qubits gates are used to implement the local terms of the Hamiltonian and if these gates have errors then we will be implementing DB-QITE with a different Hamiltonian \hat{H}' , albeit with the same locality; see Ref. [53] for a ground-state preparation DBQA which does not involve reflections but rather local diagonal Hamiltonians which are similarly robust. The energy obtained with such deformed Hamiltonian will be transparently close to the energy of the ideal implementation up to an error given by $\varepsilon = 2\|\hat{H} - \hat{H}'\|$. In particular, for stable phases of matter in condensed-matter physics applications this robustness of DB-QITE could allow for useful near-term explorations.

f. Runtime gains for QPE when warm-starting with DB-QITE. Fig. 6 showcases that using $k = 2$ steps of DB-QITE on either $|\text{Singlet}\rangle$ or $|\text{HVA}\rangle$ systematically improves the performance of QPE. Specifically for any number of precision qubits, the fidelity of QPE to the ground-state is higher when warm-starting using DB-QITE. This is the most pronounced for $k = 1$ or $k = 2$ precision qubits where the QPE output fidelity is essentially the fidelity of the initialization. For $k \geq 3$ the QPE circuits begin increasing the fidelity but warm-starting gives systematically better outputs. The gate counts shown in Fig. 6 highlight the strength of DB-QITE in that $k = 1$ or $k = 2$ steps of DB-QITE have very short runtime and so the overhead of warm-starting is very small compared to the total runtime of QPE for $k \geq 3$.

When considering warm-starting, the case of using $k = 4$ precision qubits in QPE is key. This case represents the situation where QPE is already improving the fidelity but is limited in precision from reaching the ultra-high fidelity that we find for $k = 5$. In use-cases of quantum computation such situation will be the main challenge in that circuit depth could limit QPE from running for large numbers of precision qubits because the QPE runtime grows exponentially with k . We see that for $k = 4$ an improved warm-start using DB-QITE improves QPE output to about 50% between QPE with $k = 4$ and $k = 5$. The depth cost of running QPE for $k = 5$ increases very strongly compared to $k = 4$, in contrast, the sizeable improvement using DB-QITE comes at almost no overhead in comparison.

Moreover, warm-starting with DB-QITE increases the fidelity of the initial state with the ground state, hence improves the success probability of preparing the ground state with QPE. We conclude that warm-starting using DB-QITE has a significant potential for improving the performance of QPE in practice.

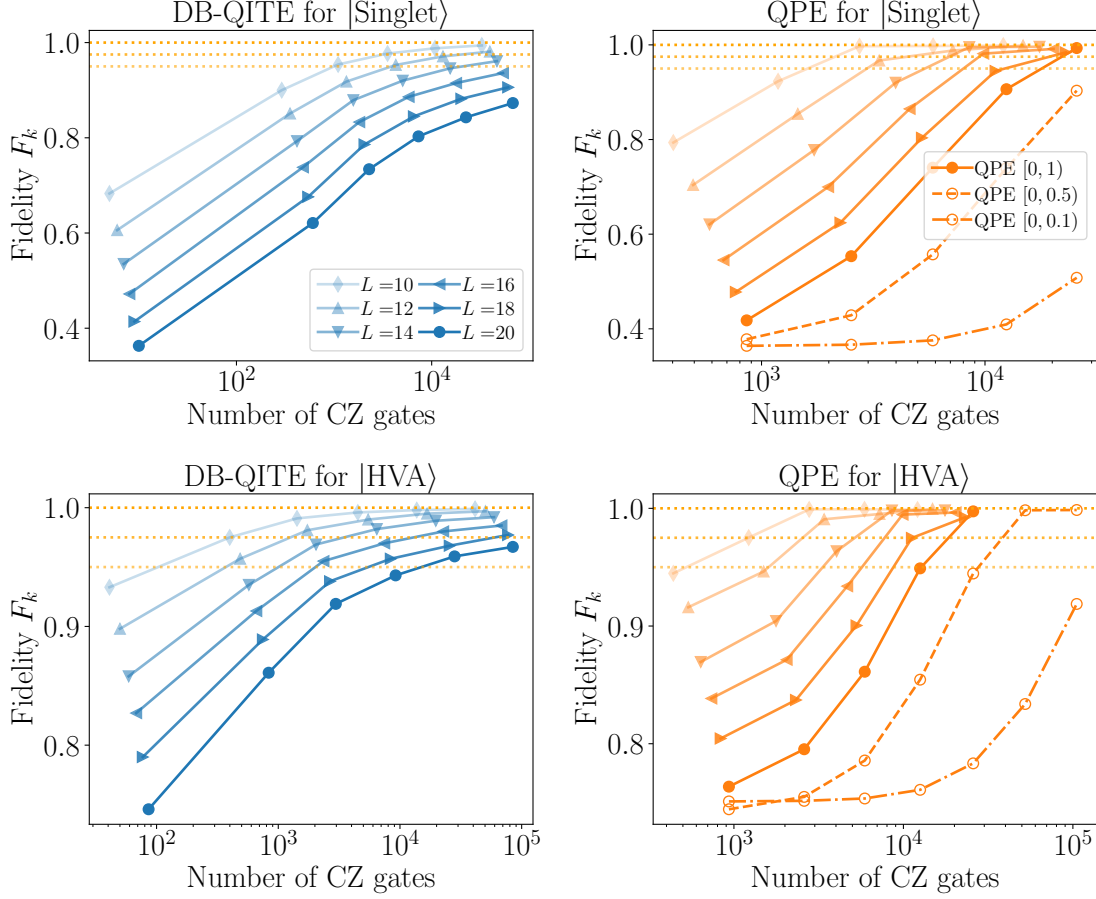


FIG. 5. Comparison between DB-QITE and QPE for L -qubit Heisenberg model for $|\text{Singlet}\rangle$ (top) and $|\text{HVA}\rangle$ (bottom) initializations. Fidelities F_k with the ground state $|\lambda_0\rangle$ and number of CZ gate are shown as a function of steps $k = 0, 1, \dots, 5$ for DB-QITE (left) and for QPE (right) as a function of the number of precision qubits $k = 1, 2, \dots, 5$. The dashed-orange lines indicate the fidelities 1.0, 0.975, 0.95. For example, for 10 qubits just $k = 4$ steps of DB-QITE are required to reach almost perfect fidelity, which is achieved with QPE with $k = 3$ precision qubits. Both methods require exponential gate counts but QPE converges faster than DB-QITE. For $|\text{HVA}\rangle$ initializations and $L = 20$ qubits, a fidelity $F \approx 95\%$ is reached with $k = 3$ steps of DB-QITE, or QPE with $k = 4$ precision qubits, requiring $N_{\text{CZ}} \approx 10^4$ CZ gates in both cases. While DB-QITE deterministically prepares the (approximate) ground state, QPE has a success probability of $P \approx 79\%$. If QPE suffers from an inaccurate spectrum rescaling to $[0, 0.5)$, the fidelity for $k = 4$ precision qubits drops to $F \approx 86\%$ and an additional precision qubit is required. In this scenario DB-QITE clearly outperforms QPE.

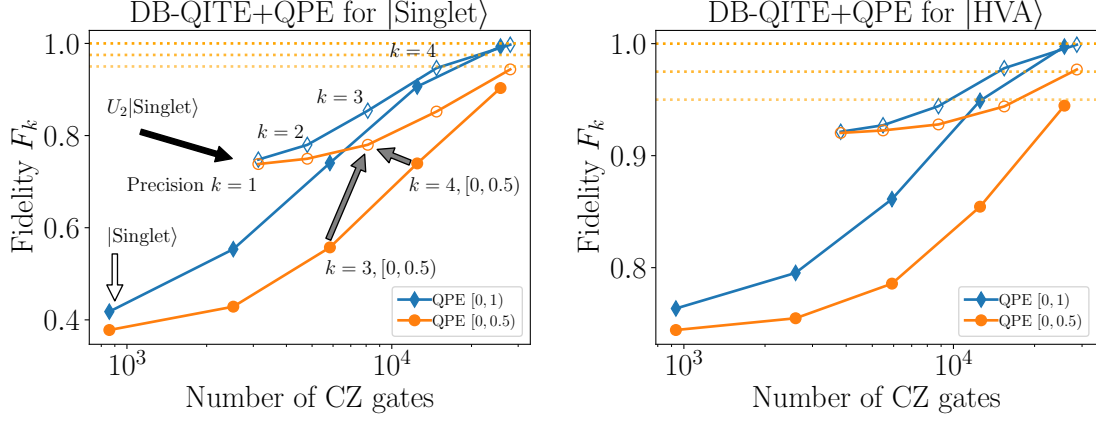


FIG. 6. Combining DB-QITE and QPE: A comparison for QPE for 20-qubit Heisenberg model with $|\text{Singlet}\rangle$, $|\text{Singlet}+\text{QITE}\rangle$ (left), $|\text{HVA}\rangle$, $|\text{HVA}+\text{QITE}\rangle$ initial states (right). Warm-starting with DB-QITE is achieved by performing $k = 2$ steps of DB-QITE from the $|\text{Singlet}\rangle$ and $|\text{HVA}\rangle$ initial states, respectively. The figures show fidelities with the ground state $|\lambda_0\rangle$ and numbers of CZ gates as a function of the number of precision qubits $k = 1, 2, \dots, 5$. The Hamiltonian \hat{H} is rescaled by an affine transformation such that the spectrum is contained in $[0, 1)$ (blue diamonds). For a more realistic scenario where the norm of the operator is not known exactly, the Hamiltonian is rescaled such that its spectrum is contained in $[0, 0.5)$ (orange circles). In this case, additional precision qubits for the QPE are required and in effect the QPE runtime in order to reach $F_k \geq 90\%$ doubles. Unless QPE has reached full precision then DB-QITE warm-start increases QPE's output fidelity. Additionally, even in the case of QPE converging onto the solution (end points of blue curves with diamonds) the warm-start should be used because it increases the success probability which is upper bounded by the initialization fidelity of QPE.